Preprints.org

Article

Not peer-reviewed version

Quantum Logical Bioinformatics: Genetic Alphabet of Four Hadamard Unitary Operators, and Cyclic Groups

S.V. Petoukhov *

Posted Date: 10 February 2026

doi: 10.20944/preprints202512.0208.v2

Keywords: quantum bioinformatics; matrix genetics; quantum logic; unitary Hadamard matrices; cycles; dual numbers; screw calculus; Fibonacci matrices; systolic processors; artificial intelligence; bioantennas; hopfion crystals

Preprints.org is a free multidisciplinary platform providing preprint service that is dedicated to making early versions of research outputs permanently available and citable. Preprints posted at Preprints.org appear in Web of Science, Crossref, Google Scholar, Scilit, Europe PMC.

Copyright: This open access article is published under a Creative Commons CC BY 4.0 license, which permit the free download, distribution, and reuse, provided that the author and preprint are cited in any reuse.

Preprints.org (www.preprints.org) | NOT PEER-REVIEWED | Posted: 10 February 2026 doi:10.20944/preprints202512.0208.v2

Disclaimer/Publisher's Note: The statements, opinions, and data contained in all publications are solely those of the individual author(s) and contributor(s) and not of MDPI and/or the editor(s). MDPI and/or the editor(s) disclaim responsibility for any injury to people or property resulting from any ideas, methods, instructions, or products referred to in the content.

Article

Quantum Logical Bioinformatics: Genetic Alphabet of Four Hadamard Unitary Operators, and Cyclic Groups

S.V. Petoukhov

Russian Engineering Academy, Russia, 125009, Moscow, Gazetny Lane, 9, Building 4; spetoukhov@gmail.com

Abstract

This article is devoted to algebraic-operator modeling of genetic informatics systems providing the inheritance of logical structures and functional algorithms. Formalisms of quantum mechanics and quantum information science are used. The author describes the identification of algebraic-operator alphabets due to algebraic analysis of structures of molecular genetic coding, which serve as the basis for developing cyclic-spiral bioinformatics. This algebraic bioinformatics exists in parallels with established biochemical informatics, which is based on the alphabets of four nucleotides in DNA and RNA and which describes the inheritance of amino acid sequences in proteins. Algebraic bioinformatics expands the possibilities for modeling the inheritance of cyclic and spiral algorithmic structures in living organisms using the formalisms of quantum information science, unitary Hadamard operators, hypercomplex dual numbers, the screw calculus, and Fibonacci matrices. The author presents genetic algebraic-operator foundations for the inheritance and modeling of a variety of geometrically regular biological forms (mollusk shells, phyllotaxis configurations, etc.). Based on the obtained results, a paradigm of code algebraic-operator Darwinism is formulated, according to which natural selection and the inheritance of the most survival-promoting code combinations of alphabetic operators of algebraic bioinformatics play an important role in evolution. This paradigm explains the rapid evolution of organisms as follows: complex tissues are formed not so much by the emergence of new genes, but by algebraic bioinformatics operators that alter the ways existing genes are used, being linked to electromagnetic waves and resonance mechanisms. The role of bioantenna arrays in the energy-informational evolution of living organisms is discussed, including the proposed biological role of hopfion crystals, which have structural analogies with the DNA double helix, as noted by the author.

Keywords: quantum bioinformatics; matrix genetics; quantum logic; unitary Hadamard matrices; cycles; dual numbers; screw calculus; Fibonacci matrices; systolic processors; artificial intelligence; bioantennas; hopfion crystals

1. Introduction

All genetically inherited physiological organs are structurally linked to the bioinformatics system of genetic texts in DNA and RNA molecules. Understanding the secrets of genetic informatics is important for the development of biotechnology, artificial intelligence, medicine, and other fields. Information communication systems are built on the use of a particular alphabet to generate information messages. For example, all computer programs rely on corresponding programming alphabets. The science of biological inheritance today is based on knowledge of the alphabets of the four nucleotides of DNA and RNA, that is, on nucleotide-alphabetic bioinformatics, which has contributed greatly to the understanding of proteins and nucleic acids. However, as Nobel laureate in chemistry T. Steitz emphasizes, all knowledge about the biochemical structure of proteins and nucleic acids encoded in the genome will not tell us, for example, how a butterfly flies [Steitz, 2007]. And they won't explain how turtles, upon hatching from its egg, immediately begin to crawl toward

© 2025 by the author(s). Distributed under a Creative Commons CC BY license.

Preprints.org (www.preprints.org) | NOT PEER-REVIEWED | Posted: 10 February 2026 doi:10.20944/preprints202512.0208.v2

the water with coordinated limb movements, which requires the logically coordinated activity of millions of their nerve and muscle cells. And they won't explain how a newborn baby emits an identification cry and begins to suckle at its mother's breast, which also requires the logically coordinated activity of billions of nerve and muscle cells. Knowledge of nucleotide sequences in DNA/RNA also doesn't deduce the inheritance of the geometrical beauty of biological forms (mollusk shells, etc.), which are repeated in organisms of very different biochemical compositions and are constructed through the spatiotemporal ordering of trillions of different molecules. Also, knowledge of the biochemical alphabet of 4 types of nucleotides does not allow us to understand how 1-dimensional sequences of nucleotides in genomic DNAs can encode the inherited 3-dimensional forms of living bodies.

Thus, the modern science of biological inheritance lacks knowledge of a bioinformatics system capable of ensuring the inheritance of "cooperative biomechanics" phenomena—the logically coordinated (coherent) behavior of body parts and the functions based on them. These inherited logical forms of collective behavior in biosystems require a search for an appropriate operator bioinformatics system based on a suitable alphabet for their modeling. It seems that, alongside nucleotide-alphabetic bioinformatics, an additional operator-alphabetic bioinformatics operates in living things. This hidden operator bioinformatics and its alphabet are apparently linked to quantum mechanics and quantum informatics, since genetic molecules belong to the microworld of quantum mechanics. In this search, special attention should be paid to unitary operators, which, as logical gates, underlie all calculations in quantum computing [Nielsen, Chuang, 2010] and which, in quantum mechanics, describe the evolution of closed quantum systems. It should be noted that the search for effective approaches to modeling logically organized biological processes is being conducted worldwide, including with reference to quantum mechanics and quantum information science, for example, in the works [Abbott, Davies, Pati, eds., 2008; Asano, Basieva, Khrennikov, et al., 2013; Khrennikov, 2004, 2006; Patel, 2001a,b; Petoukhov, Svirin, 2024].

This article is primarily devoted to the author's detection of a genetic alphabet of four Hadamard unitary operators and the development of operator quantum-logical bioinformatics based on it for the mathematical modeling of logical features of the structure and behavior of multicomponent body parts, including the characteristics of a wide set of time-coordinated cyclic processes. The article provides specific examples of modeling inherited algorithmic biological phenomena from the perspective of this emerging operator bioinformatics, which relies on the aforementioned alphabet of unitary operators, its algebraic extensions, cyclic groups of unitary operators, and quantum logic formalisms. These examples confirm the adequacy of the emerging operator bioinformatics system, which offers new approaches to modeling inherited, algorithmically organized biological phenomena, primarily those of a cyclic nature.

The founder of quantum informatics, Yu.I. Manin (https://en.wikipedia.org/wiki/Yuri_Manin), introduced the concept of a quantum computer in his book [Manin, 1980, p. 15] precisely when analyzing the characteristics of high-speed processing of information in chromosomal DNAs by "genetic automata," prophetically pointing out the important role of unitary operators and tensor products: "*A quantum automaton must be abstract: its mathematical model must use only the most general quantum principles, without prejudging physical implementations. Then the evolution model is a unitary rotation in a finite-dimensional Hilbert space, and the model of virtual separation into subsystems corresponds to the decomposition of space into a tensor product. Somewhere in this picture, there must be a place for interaction, traditionally described by Hermitian operators and probabilities*". Thus, the very birth of quantum information science, so promising for the development of artificial intelligence and quantum-logical biology, occurred thanks to the desire to understand the characteristics of genetic informatics. The data in this article are consistent with this prophecy of Yu.I. Manin.

This article also presents the detection of an algebraic-biological connection between this operator bioinformatics, based on an alphabet of 4 unitary Hadamard (2•2)-matrices, and a structurally related operator bioinformatics based on an alphabet of 4 second-order, non-unitary operators. A modeling approach based on this second operator alphabet reveals connections between

© 2025 by the author(s). Distributed under a Creative Commons CC BY license.

Preprints.org (www.preprints.org) | NOT PEER-REVIEWED | Posted: 10 February 2026 doi:10.20944/preprints202512.0208.v2

inheritance biology and the screw calculus, Fibonacci matrices, and orderly growing spiral structures that are common in nature and concern, in particular, the phyllotaxis laws of morphogenesis.

The purpose of this article is to present the results of a study of the properties and applications of the two named operator alphabets in genetics and bioinformatic systems based on them. It should be noted that the author initially discovered an operator alphabet consisting of four unitary Hadamard matrices, which later led to the identification of a related second (non-unitary) operator alphabet, also consisting of four matrix operators.

2. Genetic Matrices of DNA Nucleotide Alphabets and the Alphabet of Four Unitary Hadamard Operators for Modeling Heredity Phenomena

The amino acid sequences of proteins are inherited thanks to information messages on the genetic DNA molecules, written in the alphabet of 4 nucleotides: adenine A, cytosine C, guanine G and thymine T. This alphabet is the carrier of a system of binary-opposition indicators (molecular traits), which distinguish three types of binary sub-alphabets within it:

- 1) Two of these nucleotides are purines (A and G), having two rings in their molecule, and the other two (C and T) are pyrimidines, containing one ring. This gives a binary representation (binary sub-alphabet) **C** = **T** = **0**, **A** = **G** = **1**;

-2) two of these nucleotides are keto molecules (T and G), and the other two (C and A) are amino molecules, which gives a binary representation **C** = **A** = **0**, **T** = **G** = **1**;

-3) pairs of complementary nucleotides A-T and C-G are linked by 2 and 3 hydrogen bonds, respectively (called weak and strong hydrogen bonds in genetics), which gives a binary representation **C** = **G** = **0**, **A** = **T** = **1**.

These binary features of the nucleotide alphabet of DNA (and RNA) of all living organisms are summarized in Table 1 of the distribution of features in it.

Table 1. Distribution of binary molecular features in the DNA alphabet of 4 nucleotides G, A, T, C, where binary oppositions designated by the symbols +1 and -1. The fourth row of the table represents the presence of benzene rings in the molecules of all four nucleotides with the symbol +1.

Molecular traits and their symbols	G	A	T	C
Pyrimidines +1, purines -1	-1	-1	+1	+1
Amino-nucleotides +1, keto-nucleotides -1	-1	+1	-1	+1
Complementarity with 3 or 2 hydrogen bonds: +1, -1	+1	-1	-1	+1
The presence of benzene rings +1	+1	+1	+1	+1

On the right-hand side of this phenomenological Table 1, a symmetrical Hadamard (4•4)-matrix emerged, which is real Hermitian matrix, whose quadrants are occupied by four types of Hadamard (2•2)-matrices. Recall that Hadamard matrices H_n of order n are square matrices composed of elements +1 and -1 satisfying the criterion $H_n \bullet H_n^T = n \bullet E$, where E is the identity matrix of order n. Figure 1 shows these four second-order Hadamard matrices from Table 1, normalized by a factor of $2^{-0.5}$, traditionally used in quantum mechanics and quantum computers to impart a unitary character to Hadamard matrices. Hadamard matrices have many remarkable properties and applications (see, for example, [Balonin, Sergeev, 2024]).

$$\mathbf{H_C} = 2^{-0.5}\begin{vmatrix} 1, -1 \\ 1, 1 \end{vmatrix};\quad \mathbf{H_T} = 2^{-0.5}\begin{vmatrix} 1, 1 \\ 1, -1 \end{vmatrix};\quad \mathbf{H_G} = 2^{-0.5}\begin{vmatrix} 1, 1 \\ -1, 1 \end{vmatrix};\quad \mathbf{H_A} = 2^{-0.5}\begin{vmatrix} -1, 1 \\ 1, 1 \end{vmatrix}$$

Figure 1. Four unitary Hadamard matrices $\mathbf{H_C}$, $\mathbf{H_A}$, $\mathbf{H_T}$, and $\mathbf{H_G}$.

© 2025 by the author(s). Distributed under a Creative Commons CC BY license.

Preprints.org (www.preprints.org) | NOT PEER-REVIEWED | Posted: 10 February 2026 doi:10.20944/preprints202512.0208.v2

Identifying this relationship between the DNA nucleotide alphabet and these four unitary Hadamard matrices is important due to the significance of unitary transformations (unitary operators) for quantum mechanics, quantum computing, biosystems, signal processing engineering, and other fields. Unitary transformations preserve vector lengths and dot products (preserve the metric), representing rotation and mirror reflection operators. Unitary matrices satisfy the criterion: the product of a unitary matrix with its transpose is equal to one. Unitary transformations with real components are called orthogonal transformations, but in this article, we will use their more general name, "unitary transformations," by which they are better known in various fields of science. In quantum mechanics, unitary transformations describe the time evolution of closed quantum systems. In quantum mechanics (unlike classical mechanics), observable quantities are represented by operators rather than numbers. In quantum computers, all calculations are performed using unitary operators, which act as logical gates, and any unitary operator can be used as a gate in quantum computing [Nielsen, Chuang, 2010]. Hadamard matrices are fundamental building blocks of quantum computers, enabling qubit superposition and are also a key element of quantum parallelism in the quantum Fourier transform and other quantum algorithms.

We will call the four unitary operators $\mathbf{H}_C$, $\mathbf{H}_A$, $\mathbf{H}_T$, and $\mathbf{H}_G$ (Figure 1) genetic Hadamard gates and consider them the desired quantum operator alphabet, which forms the basis of a quantum-logical bioinformatics system for modeling the heritable phenomena of cooperative biomechanics. These four matrices cyclically transform into each other when they are rotated by 90 degrees. This same set of four Hadamard matrices is identified in the analysis of molecular genetic informatics from other approaches. For example, the binary molecular features indicated in Table 1 allow these 4 alphabetic nucleotides to be placed in four possible variants of (2×2)-matrices, the rows of which are numbered with the binary numbers 0 and 1 of one binary sub-alphabet (for example, the sub-alphabet of amino-nucleotides and keto-nucleotides C = A = 0, T = G = 1), and the columns with the binary numbers 0 and 1 of another sub-alphabet (for example, the sub-alphabet of pyrimidines and purines C = T = 0, A = G = 1) (Figure 2). In such a matrix, all 4 nucleotides C, A, T, G occupy an individual place, since from the point of view of these two sub-alphabets, nucleotide C receives the binary number **00**, nucleotide A - the binary number **01**, nucleotide T - the binary number **10**, nucleotide G - the binary number **11** (the first binary symbol of the nucleotide is taken from the number of its row, and the second - from the number of its column).

	0	1
0	C	A
1	T	G

	1	0
0	A	C
1	G	T

	1	0
1	G	T
0	A	C

	0	1
1	T	G
0	C	A

Figure 2. All 4 possible arrangements of 4 nucleotides C, A, G, T in genetic (2•2)-matrices, the rows of which are numbered by binary numbers of the sub-alphabet of amino nucleotides (C, A) and keto nucleotides (T, G), and the columns by binary numbers of the sub-alphabet of pyrimidines (C, T) and purines (A, G).

But in the DNA alphabet of 4 nucleotides, nature has built in another binary opposition: during the transition from DNA to RNA, only one nucleotide T (thymine) is replaced by the nucleotide U (uracil), while the remaining nucleotides C, A, G remain unchanged. This binary opposition is expressed by the representation: C = A = G = +1, T = -1. Taking this binary representation into account transforms the 4-symbol genetic matrices from Figure 2 into 4 numerical matrices in Figure 3, which are the same Hadamard matrices discussed above in connection with Figure 1 and which become unitary matrices $\mathbf{H}_C$, $\mathbf{H}_A$, $\mathbf{H}_T$, and $\mathbf{H}_G$ under the same normalization by multiplying by a factor of $2^{-0.5}$.

© 2025 by the author(s). Distributed under a Creative Commons CC BY license.

Preprints.org (www.preprints.org) | NOT PEER-REVIEWED | Posted: 10 February 2026 doi:10.20944/preprints202512.0208.v2

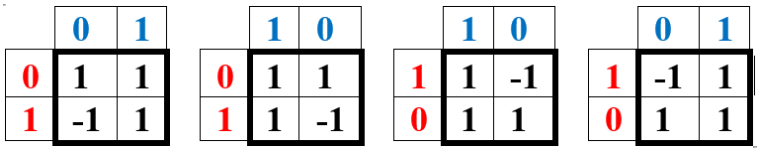

Figure 3. A set of 4 numerical Hadamard matrices arising from the 4 symbolic genetic matrices in Figure 2, taking into account the genetic binary opposition of the nucleotide T to the nucleotides A, C, G, giving the binary representation: C = A = G = +1, T = -1.

Let us briefly mention that similar Hadamard (2•2)-matrices are also revealed under other types of analysis of structural and stochastic features of genetic informatics. For example, taking into account the well-known second Chargaff rule [Fimmel, Gumbel, Karpuzoglu, Petoukhov, 2019; Yamagishi, 2017] on the ratio of probabilities of 4 nucleotides in all long single-stranded DNAs (length greater than 100 kilobits) of higher and lower organisms leads to a real Hermitian probability matrix $\mathbf{W}_D$ = [0.5, 0.5; 0.5, 0.5]. This genetic Hermitian matrix $\mathbf{W}_D$ is doubly stochastic: the sum of the elements in each row and each column of such a matrix is equal to one. However, the following theorem is known regarding doubly stochastic matrices [Prasolov, 2008]:

- If the matrix $\mathbf{V} = ||\mathbf{v}_{ij}||^n$ is unitary, then the matrix $\mathbf{W} = ||\mathbf{w}_{ij}||^n$, where $\mathbf{w}_{ij} = |\mathbf{v}_{ij}|^2$, is doubly stochastic. является дважды стохастической.

According to this theorem, the specified doubly stochastic genetic matrix $\mathbf{W}_D$ of probabilities corresponds to four unitary alphabetic Hadamard matrices $\mathbf{H}_C$, $\mathbf{H}_A$, $\mathbf{H}_T$, and $\mathbf{H}_G$ from Figure 1: squaring all components of each of these unitary matrices generates the doubly stochastic matrix $\mathbf{W}_D$. Note that these same four unitary matrices $\mathbf{H}_C$, $\mathbf{H}_A$, $\mathbf{H}_T$, and $\mathbf{H}_G$, but taken with a minus sign, are treated as their banal analog and are not considered separately. The totality of the obtained results of the analysis of molecular genetic informatics allows us speaking about the fundamental bioinformatic significance of these alphabetic unitary Hadamard matrices for the bioinformatic coding of inherited biological phenomena associated with the ideology of closed quantum-like biosystems. These include inherited cyclical and biorhythmic phenomena, which, as will be shown below, are effectively modeled based on the use of these unitary matrices.

One of these four Hadamard genetic unitary operators (gates) - the $\mathbf{H}_T$ - has long been used in quantum computers for fundamental operations on qubits, serving as a key element in many quantum algorithms, including the Deutsch-Jozsa algorithm and Shor's algorithm. This Hadamard gate provides quantum algorithms with a superposition principle for dealing with quantum entanglement, demonstrating quantum superiority—their significantly more efficient operation compared to known classical algorithms [Nielsen, Chuang, 2010].

Of the four genetic Hadamard gates, two gates $\mathbf{H}_A$, $\mathbf{H}_T$ are mirror reflection operators. Raising them to integer powers generates the corresponding cyclic groups of unitary operators with period 2. The other two unitary matrices ($\mathbf{H}_C$, $\mathbf{H}_G$) are rotation operators ($\mathbf{H}_C$ counterclockwise, $\mathbf{H}_G$ clockwise) and matrix representations of the complex number $Z = (1+i)\bullet 2^{-0.5}$, where i is the imaginary unit of the complex number ($i^2 = -1$). Repeated raising these unitary matrices $\mathbf{H}_C$ and $\mathbf{H}_G$ to integer powers (positive and negative) generates cyclic (with period 8) groups of unitary operators, which are matrix representations of the complex numbers (1).

$$\mathbf{H}_C^n = \mathbf{H}_C^{n+8},\ \mathbf{H}_G^n = \mathbf{H}_G^{n+8},\ \mathbf{H}_A^n = \mathbf{H}_A^{n+2},\ \mathbf{H}_T^n = \mathbf{H}_T^{n+2} \quad (1)$$

Besides this, any of the unitary matrices $\mathbf{H}_C$ and $\mathbf{H}_G$ can be represented as the product of k unitary matrices, which are their kth roots. In other words, the action of a single unitary operator, for example, $\mathbf{H}_C$, can be represented as the action of a sequence of k smaller unitary operators $\mathbf{H}_C\mathbf{1/k}$. Thus, with the matrix-vector approach, any large transformation in the system from the action of such a large operator $\mathbf{H}_C$ can be represented as consisting of a sequence of arbitrarily small transformations from the action of the corresponding sequence of unitary operators $\mathbf{H}_C\mathbf{1/k}$. for

© 2025 by the author(s). Distributed under a Creative Commons CC BY license.

Preprints.org (www.preprints.org) | NOT PEER-REVIEWED | Posted: 10 February 2026 doi:10.20944/preprints202512.0208.v2

modeling quasi-continuous transformations in the simulated cyclic processes. We also note that raising the genetic gate $\mathbf{H}_C$ or $\mathbf{H}_G$ to a power representing the cycle-by-cycle cyclic function of time allows modeling quasi-continuous cyclic bioprocesses as vector sequences of their cycle-by-cycle states.

Projectors (projection operators) play an important role in quantum logic. In light of this, we note that the unitary Hadamard matrices $\mathbf{H}_C$ and $\mathbf{H}_G$ are sums of two sparse matrices, which are shown in parentheses in expression (2) and which represent projectors $\mathbf{P}_s$ satisfying the projection criterion $\mathbf{P}_s^2 = \mathbf{P}_s$:

$$\mathbf{H}_C = 2^{-0.5} \bullet [1\ -1;\ 1\ 1] = 2^{-0.5} \bullet ([1,\ 0;\ 1,\ 0] + [0,\ -1;\ 0,\ 1]),$$

$$\mathbf{H}_G = 2^{-0.5} \bullet [1\ 1;\ -1\ 1] = 2^{-0.5} \bullet ([1,\ 0;\ -1,\ 0] + [0,\ 1;\ 0,\ 1]) \quad (2)$$

Many genetically inherited biological structures in organisms are clearly linked to unitary transformations of rotations and of mirror images. For example, the kinematic schema of the human body and its locomotion is based on unitary transformations of rotations at the joints (the human body has approximately 300 joints) and of mirror symmetry of the left and right halves of the body. Human motor activity is reduced to the skillful control by the nervous system of ensembles of these unitary transformations in the kinematics of the body, which is associated with the genetically inherited ability of the nervous system to operate unitary transformations. Moreover, a person's very concept of their body schema is innate: people with limbs missing from birth and no personal experience using them nevertheless perceive them as truly existing, with phantom pain in them [Vetter, Weinstein, 1967; Weinstein, Sersen, 1961].

When studying human sensorimotor characteristics, it's important to consider that the genetically inherited nervous system is related to genetic structures. Humans perceive the world through probabilities in statistical streams of signals from neurons in the retina (containing millions of receptor cells) and other sensory organs. Norbert Wiener, the father of cybernetics, asserted: "Genetic memory—the memory of our genes—is essentially determined by nucleic acid complexes...there is reason to believe that the memory of the nervous system is of the same nature" [Wiener, 1964; Rebrova I., Rebrova O., 2020].

Another example of the biological importance of unitary transformations is the construction of complex three-dimensional protein shapes in the body, known as protein folding. These shapes are based on unitary transformations involving the rotation of protein molecule segments relative to each other around relatively strong carbon-carbon bonds.

The author proposes to consider and use the family of 4 genetic unitary Hadamard operators $\mathbf{H}_C$, $\mathbf{H}_A$, $\mathbf{H}_T$, $\mathbf{H}_G$ (Figure 1) as a basic genetic quantum-logical alphabet for the development on its basis of the theory of a quantum-logical bioinformation system of unitary type that allows modeling some genetically inherited and algorithmically organized biological structures and phenomena, primarily of a cyclical and rhythmic nature.

Here, the distinctive features of quantum logic should be clarified [Cohen, 1989; Vasyukov, 2005]. From a formal point of view, quantum logic is an algebraic system for describing, using quantum gates, how qubits operate and interact and how to extract information from them. In quantum logic, "logic" is not contained in reasoning, but in the mathematical description of states and operations. Quantum logic can be formulated as a modified version of propositional logic. For comparison, we recall that classical Boolean logic is a set of logical rules (AND, OR, NOT, etc.) describing how bits (0 or 1) can be combined and transformed according to the laws of Boolean algebra with its key principle of distributivity and the statements "true" or "false." Quantum logic considers not "true/false" statements, but questions about a quantum system. The answer to this question is provided by the probability value obtained during the measurement. Logical operations are replaced by quantum gates (unitary operations): NOT becomes an X gate, and completely new operations emerge that have no analogues in classical logic, such as the Hadamard gate, which creates

© 2025 by the author(s). Distributed under a Creative Commons CC BY license.

Preprints.org (www.preprints.org) | NOT PEER-REVIEWED | Posted: 10 February 2026 doi:10.20944/preprints202512.0208.v2

superposition. Quantum logic operates on qubits, vectors, and matrices rather than sets. Its mathematical foundation is the theory of Hilbert spaces and unitary and projective operators. The state space of a quantum system is described by vectors, and rotations of these vectors serve as logical operations. Quantum logic lacks distributivity, which is considered its key difference from Boolean logic. Quantum logic is a branch of logic necessary for reasoning about propositions that respect the principles of quantum theory. It was founded by the work of G. Birkhoff and J. von Neumann [Birkhoff, von Neumann, 1936], who sought to reconcile the inconsistencies of classical logic with the facts about measurements in quantum mechanics and saw in quantum logic a possible foundation for physics.

The unitary Hadamard matrices of the quantum operator alphabet $\mathbf{H}_C$, $\mathbf{H}_A$, $\mathbf{H}_T$, $\mathbf{H}_G$ of bioinformatics (Figure 1) and many types of their combinations into unitary matrices of higher orders form—when repeatedly raised to powers—cyclic groups of operators with different periods and used to model cyclic sequences of states of quantum-like systems. The resulting algebraic-geometric apparatus is intended, first of all, for quantum-logical modeling of a variety of genetically inherited cyclic and hypercyclic biostructures in genetic biomechanics. It should be noted that the quantum-logical approach to inherited cyclic and hypercyclic biostructures developed by the author, based on the alphabet of genetic Hadamard gates and the mathematical apparatus of quantum-logical biology, differs fundamentally from the well-known biochemical concept of catalytic cycles and hypercycles [Eigen, Schuster, 1979].

World research in genetic informatics relies heavily on the fundamental fact that the DNA of all organisms contains a molecular alphabet of 4 nucleotides: C, G, A, T, and its extensions into alphabets of 16 duplets, 64 triplets, and so on. In parallel with this molecular alphabet of 4 nucleotides, bioinformatics and genetic biomechanics now can work with an operator alphabet of 4 genetic Hadamard gates, that is, a fundamentally new type of alphabet: a quantum-logical operator-code alphabet of 4 unitary matrices: $\mathbf{H}_C$, $\mathbf{H}_A$, $\mathbf{H}_T$, $\mathbf{H}_G$. This alphabet gives rise to interconnected sets of higher-order unitary operators, providing new approaches for modeling, primarily, inherited cyclical and biorhythmic phenomena.

These genetic unitary Hadamard matrices are conjugated with the corresponding complete orthogonal systems of Walsh functions. The latter are the basis of a special spectral analysis of signals in digital information technology and are associated with cyclic Gray codes, logical holography, Walsh antennas, and the fractal Hilbert curve, which is known to correspond to the spatial packing of chromatin in the human genome [Lieberman-Aiden et al., 2009]. The relationship of Hadamard matrices with the listed scientific tools is described in our works [Petoukhov, 2008; Petoukhov, 2024a,b; Petoukhov, He, 2023].

The mathematical properties of the alphabet of 4 genetic unitary Hadamard matrices and the sets of unitary operators constructed on their basis are subject to systematic study. For example, the non-zero commutators among these unitary operators are subject to study (in quantum mechanics, the study of pairs of operators characterized by non-zero commutators led to the formulation of the Heisenberg uncertainty principle). Already in the alphabet of 4 genetic Hadamard gates, there are three pairs of non-commuting unitary operators characterized by non-zero commutators (3); the values of these commutators are equal in two cases to Hadamard matrices, and in the third to the matrix representation of twice the imaginary unit i of a complex number:

$$\mathbf{H}_A \bullet \mathbf{H}_C - \mathbf{H}_C \bullet \mathbf{H}_A = [1, 1; 1, -1],$$

$$\mathbf{H}_C \bullet \mathbf{H}_T - \mathbf{H}_T \bullet \mathbf{H}_C = [-1, 1; 1, 1],$$

$$\mathbf{H}_A \bullet \mathbf{H}_T - \mathbf{H}_T \bullet \mathbf{H}_A = [0, -2; 2, 0] \quad (3)$$

© 2025 by the author(s). Distributed under a Creative Commons CC BY license.

Preprints.org (www.preprints.org) | NOT PEER-REVIEWED | Posted: 10 February 2026 doi:10.20944/preprints202512.0208.v2

At this stage of research, the question of the genetic significance and possible interpretation of these and other facts about non-zero commutators among genetic unitary operators remains open for discussion.

The next section examines the development of the mathematical apparatus of quantum-logical bioinformatics, which includes a variety of genetic unitary operators and their cyclic groups for modeling genetically inherited cyclic biostructures and biorhythmic processes.

3. Expandable Set of Genetic Unitary Operators and Their Cyclic Groups

The DNA alphabet of 4 nucleotides C, A, T, G is identical in the number of elements to the quantum-logical alphabet of 4 genetic Hadamard gates $\mathbf{H_C}$, $\mathbf{H_A}$, $\mathbf{H_T}$, and $\mathbf{H_G}$ (Figure 3). In matrix genetics, it is known that, based on the genetic (2•2)-matrix of the alphabet of 4 nucleotides, by raising it to tensor powers, genetic (2^n•2^n)-matrices are formed with a strictly regular arrangement of 16 duplets, 64 triplets, 256 tetraplets, etc., respectively [Petoukhov, 2008; Petoukhov, He, 2023]. Figure 4 shows examples from these books of genetic matrices of 4 nucleotides, 16 duplets and 64 triplets obtained in this tensor way.

	0	1
0	C	A
1	T	G

;

	00	01	10	11
00	CC	CA	AC	AA
01	CT	CG	AT	AG
10	TC	TA	GC	GA
11	TT	TG	GT	GG

	000	001	010	011	100	101	110	111
000	CCC	CCA	CAC	CAA	ACC	ACA	AAC	AAA
001	CCT	CCG	CAT	CAG	ACT	ACG	AAT	AAG
010	CTC	CTA	CGC	CGA	ATC	ATA	AGC	AGA
011	CTT	CTG	CGT	CGG	ATT	ATG	AGT	AGG
100	TCC	TCA	TAC	TAA	GCC	GCA	GAC	GAA
101	TCT	TCG	TAT	TAG	GCT	GCG	GAT	GAG
110	TTC	TTA	TGC	TGA	GTC	GTA	GGC	GGA
111	TTT	TTG	TGT	TGG	GTT	GTG	GGT	GGG

Figure 4. Tensor family of genetic matrices of 4 nucleotides C, A, T, G, 16 duplets, and 64 triplets.

The tensor product is a critical operation in the quantum mechanics of multicomponent systems and quantum information science [Nielsen, Chuang, 2010]. By analogy with the tensor family of genetic matrices based on the alphabet of 4 nucleotides (Figure 4), we construct a tensor family of genetic matrices based on the alphabet of 4 Hadamard genetic gates $\mathbf{H_C}$, $\mathbf{H_A}$, $\mathbf{H_T}$, and $\mathbf{H_G}$ (Figure 3), for example, by simply replacing the nucleotide symbols C, A, T, and G with similarly indexed symbols of these gates and connecting neighbor gates in a bundle with the tensor multiplication symbol ⊗ (Figure 5).

$\mathbf{H_C}$	$\mathbf{H_A}$
$\mathbf{H_T}$	$\mathbf{H_G}$

;

$\mathbf{H_C}\otimes\mathbf{H_C}$	$\mathbf{H_C}\otimes\mathbf{H_A}$	$\mathbf{H_A}\otimes\mathbf{H_C}$	$\mathbf{H_A}\otimes\mathbf{H_A}$
$\mathbf{H_C}\otimes\mathbf{H_T}$	$\mathbf{H_C}\otimes\mathbf{H_G}$	$\mathbf{H_A}\otimes\mathbf{H_T}$	$\mathbf{H_A}\otimes\mathbf{H_G}$
$\mathbf{H_T}\otimes\mathbf{H_C}$	$\mathbf{H_T}\otimes\mathbf{H_A}$	$\mathbf{H_G}\otimes\mathbf{H_C}$	$\mathbf{H_G}\otimes\mathbf{H_A}$
$\mathbf{H_T}\otimes\mathbf{H_T}$	$\mathbf{H_T}\otimes\mathbf{H_G}$	$\mathbf{H_G}\otimes\mathbf{H_T}$	$\mathbf{H_G}\otimes\mathbf{H_G}$

$H_C\otimes H_C\otimes H_C$	$H_C\otimes H_C\otimes H_A$	$H_C\otimes H_A\otimes H_C$	$H_C\otimes H_A\otimes H_A$	$H_A\otimes H_C\otimes H_C$	$H_A\otimes H_C\otimes H_A$	$H_A\otimes H_A\otimes H_C$	$H_A\otimes H_A\otimes H_A$
$H_C\otimes H_C\otimes H_T$	$H_C\otimes H_C\otimes H_G$	$H_C\otimes H_A\otimes H_T$	$H_C\otimes H_A\otimes H_G$	$H_A\otimes H_C\otimes H_T$	$H_A\otimes H_C\otimes H_G$	$H_A\otimes H_A\otimes H_T$	$H_A\otimes H_A\otimes H_G$
$H_C\otimes H_T\otimes H_C$	$H_C\otimes H_T\otimes H_A$	$H_C\otimes H_G\otimes H_C$	$H_C\otimes H_G\otimes H_A$	$H_A\otimes H_T\otimes H_C$	$H_A\otimes H_T\otimes H_A$	$H_A\otimes H_G\otimes H_C$	$H_A\otimes H_G\otimes H_A$
$H_C\otimes H_T\otimes H_T$	$H_C\otimes H_T\otimes H_G$	$H_C\otimes H_G\otimes H_T$	$H_C\otimes H_G\otimes H_G$	$H_A\otimes H_T\otimes H_T$	$H_A\otimes H_T\otimes H_G$	$H_A\otimes H_G\otimes H_T$	$H_A\otimes H_G\otimes H_G$
$H_T\otimes H_C\otimes H_C$	$H_T\otimes H_C\otimes H_A$	$H_T\otimes H_A\otimes H_C$	$H_T\otimes H_A\otimes H_A$	$H_G\otimes H_C\otimes H_C$	$H_G\otimes H_C\otimes H_A$	$H_G\otimes H_A\otimes H_C$	$H_G\otimes H_A\otimes H_A$
$H_T\otimes H_C\otimes H_T$	$H_T\otimes H_C\otimes H_G$	$H_T\otimes H_A\otimes H_T$	$H_T\otimes H_A\otimes H_G$	$H_G\otimes H_C\otimes H_T$	$H_G\otimes H_C\otimes H_G$	$H_G\otimes H_A\otimes H_T$	$H_G\otimes H_A\otimes H_G$
$H_T\otimes H_T\otimes H_C$	$H_T\otimes H_T\otimes H_A$	$H_T\otimes H_G\otimes H_C$	$H_T\otimes H_G\otimes H_A$	$H_G\otimes H_T\otimes H_C$	$H_G\otimes H_T\otimes H_A$	$H_G\otimes H_G\otimes H_C$	$H_G\otimes H_G\otimes H_A$
$H_T\otimes H_T\otimes H_T$	$H_T\otimes H_T\otimes H_G$	$H_T\otimes H_G\otimes H_T$	$H_T\otimes H_G\otimes H_G$	$H_G\otimes H_T\otimes H_T$	$H_G\otimes H_T\otimes H_G$	$H_G\otimes H_G\otimes H_T$	$H_G\otimes H_G\otimes H_G$

Figure 5. Tensor family of matrices of 4 genetic Hadamard gates $\mathbf{H_C}$, $\mathbf{H_A}$, $\mathbf{H_T}$, $\mathbf{H_G}$, 16 duplets, and 64 triplets of these gates.

© 2025 by the author(s). Distributed under a Creative Commons CC BY license.

Preprints.org (www.preprints.org) | NOT PEER-REVIEWED | Posted: 10 February 2026 doi:10.20944/preprints202512.0208.v2

We emphasize that the tensor product of unitary Hadamard operators always yields a unitary Hadamard operator of increased order, conjugate, as noted above, with the corresponding complete orthogonal system of Walsh functions, cyclic Gray codes, fractal Hilbert curves, logical holography, Walsh antennas, etc. [Petoukhov, 2024a,b]. Accordingly, the content of each cell in the $(2^n \bullet 2^n)$-matrices of the tensor family $[\mathbf{H_C}, \mathbf{H_A}; \mathbf{H_T}, \mathbf{H_G}]^{(n)}$ is a unitary Hadamard operator of the corresponding order. Raising each of these Hadamard gates to an integer power generates a cyclic group of unitary operators characterized by a certain period. It can be shown that the periods of all cyclic groups of gates within each of the matrices of this tensor family are interconnected on the basis of multidimensional hypercomplex numbers. We demonstrate this using the example of the first two matrices of the tensor family of matrices under consideration, located in Figure 5 at the top.

The cyclic groups based on raising the terms of the matrix 4 of the alphabetic gates $\mathbf{H_C}$, $\mathbf{H_A}$, $\mathbf{H_T}$, $\mathbf{H_G}$ to integer powers n have periods of 8 and 2, as indicated above in expression (1). Figure 6 shows a representation of this matrix from Figure 5 as a matrix of periods **R**, which indicates the values of the periods of the cyclic groups of each of these genetic gates. It is also shown that this matrix of periods **R** is the sum of two sparse matrices $\mathbf{r_0}$ and $\mathbf{r_1}$ with weight coefficients of 8 and 2. But the set of these matrices $\mathbf{r_0}$ and $\mathbf{r_1}$ is closed with respect to multiplication and determines the table of their multiplication (Figure 6 below), which is known in mathematics as the multiplication table of basic elements of the algebra of 2-dimensional hyperbolic numbers [Kantor, Solodovnikov, 1973; Petoukhov, 2008]. This means that the matrix **R** is a matrix representation of the 2-dimensional hyperbolic number 8+2j, where j is the imaginary unit of the hyperbolic number.

$$\begin{bmatrix} \mathbf{H_C} & \mathbf{H_A} \\ \mathbf{H_T} & \mathbf{H_G} \end{bmatrix} \rightarrow \mathbf{R} = \begin{bmatrix} 8 & 2 \\ 2 & 8 \end{bmatrix} = 8 \begin{bmatrix} 1, 0 \\ 0, 1 \end{bmatrix} + 2 \begin{bmatrix} 0, 1 \\ 1, 0 \end{bmatrix} = 8\mathbf{r_0} + 2\mathbf{r_1}$$

•	$\mathbf{r_0}$	$\mathbf{r_1}$
$\mathbf{r_0}$	$\mathbf{r_0}$	$\mathbf{r_1}$
$\mathbf{r_1}$	$\mathbf{r_1}$	$\mathbf{r_0}$

Figure 6. Representation of the matrix of 4 Hadamard gates $\mathbf{H_C}$, $\mathbf{H_A}$, $\mathbf{H_T}$, $\mathbf{H_G}$ from Figure 5 in the form of a matrix **R** of periods 8 and 2 corresponding cyclic groups based on raising these gates to integer powers n: $\mathbf{H_C^n}$, $\mathbf{H_A^n}$, $\mathbf{H_T^n}$, $\mathbf{H_G^n}$. Also shown are the decomposition of this matrix **R** into the sum of two sparse matrices $8\mathbf{r_0} + 2\mathbf{r_1}$ and the multiplication table of the matrices $\mathbf{r_0}$ and $\mathbf{r_1}$, which coincides with the multiplication table of the algebra of 2-dimensional hyperbolic numbers.

Let us now turn to the matrix of 16 tensor duplets of Hadamard gates from Figure 5. The cyclic groups based on raising the terms of this matrix to integer powers have periods of 2, 4, and 8. Figure 7 shows the (4•4)-matrix $\mathbf{R_2}$, representing the named matrix of unitary operators as a matrix of periods of the corresponding cyclic groups of its 16 terms. This matrix $\mathbf{R_2}$ is a bisymmetric Hermitian real matrix. The sums of the components in each of its rows and columns are equal (with appropriate normalization, it becomes a doubly stochastic matrix). As shown in Figure 7, the matrix $\mathbf{R_2}$ is the sum of 4 sparse matrices $\mathbf{s_0}$, $\mathbf{s_1}$, $\mathbf{s_2}$, $\mathbf{s_3}$ (the numbering corresponds to the order of their sequence in Figure 7 from left to right) with weight coefficients 4, 8, 8, 2. The set of these 4 sparse matrices is closed under multiplication and determines the table of their multiplication, known in mathematics as the multiplication table of basic elements of the algebra of 4-dimensional hyperbolic numbers [Kantor, Solodovnikov, 1973; Petukhov, 2008]. This means that the matrix of periods of the considered cyclic groups of unitary operators $\mathbf{R_2}$ is a matrix representation of the 4-dimensional hyperbolic number $4+8k_1+8k_2+2k_3$, where k_1, k_2, k_3 are imaginary units of 4-dimensional hyperbolic numbers.

© 2025 by the author(s). Distributed under a Creative Commons CC BY license.

Preprints.org (www.preprints.org) | NOT PEER-REVIEWED | Posted: 10 February 2026 doi:10.20944/preprints202512.0208.v2

$$\mathbf{R}_2 = \begin{bmatrix} 4 & 8 & 8 & 2 \\ 8 & 4 & 2 & 8 \\ 8 & 2 & 4 & 8 \\ 2 & 8 & 8 & 4 \end{bmatrix} = 4\begin{bmatrix} 1 & 0 & 0 & 0 \\ 0 & 1 & 0 & 0 \\ 0 & 0 & 1 & 0 \\ 0 & 0 & 0 & 1 \end{bmatrix} + 8\begin{bmatrix} 0 & 1 & 0 & 0 \\ 1 & 0 & 0 & 0 \\ 0 & 0 & 0 & 1 \\ 0 & 0 & 1 & 0 \end{bmatrix} + 8\begin{bmatrix} 0 & 0 & 1 & 0 \\ 0 & 0 & 0 & 1 \\ 1 & 0 & 0 & 0 \\ 0 & 1 & 0 & 0 \end{bmatrix} + 2\begin{bmatrix} 0 & 0 & 0 & 1 \\ 0 & 0 & 1 & 0 \\ 0 & 1 & 0 & 0 \\ 1 & 0 & 0 & 0 \end{bmatrix}$$

•	S_0	S_1	S_2	S_3
S_0	S_0	S_1	S_2	S_3
S_1	S_1	S_0	S_3	S_2
S_2	S_2	S_3	S_0	S_1
S_3	S_3	S_2	S_1	S_0

Figure 7. The matrix $\mathbf{R}_2$ of the periods of 16 cyclic groups, representing the matrix of 16 tensor duplets in Figure 5, is the sum of the four sparse matrices $\mathbf{s}_0$, $\mathbf{s}_1$, $\mathbf{s}_2$, $\mathbf{s}_3$ shown with their weight coefficients. The multiplication table of these sparse matrices is shown as well.

In the general case, such a tensor family of $(2^n \bullet 2^n)$-matrices $[\mathbf{H}_C, \mathbf{H}_A; \mathbf{H}_T, \mathbf{H}_G]^{(n)}$, obtained by raising the original alphabetic matrix of 4 Hadamard gates to the tensor power (n), contains 4^n unitary operators, each of which, when raised to an integer power, generates its own cyclic group of unitary operators with a certain period. A detailed analysis of the set of these tensor-generated Hadamard unitary operators should be conducted in the future, including the study of their transformations under cyclic permutations of their columns and rows, as well as the study of commutators between individual operators, etc.

In addition to the described tensor generation of new unitary operators based on the genetic alphabet of four Hadamard gates, there is another approach to their formation. This involves constructing multiblock matrices whose blocks are the alphabetic Hadamard gates $\mathbf{H}_C$, $\mathbf{H}_A$, $\mathbf{H}_T$, $\mathbf{H}_G$. Figure 8 shows an example of a block unitary operator constructed in this way from a combination of all four of these gates, which is also a Hadamard operator with a weighting factor of 0.5.

$$\mathbf{Z} = 2^{-0.5}\begin{bmatrix} \mathbf{H}_C & -\mathbf{H}_A \\ \mathbf{H}_T & \mathbf{H}_G \end{bmatrix} = 0.5\begin{bmatrix} 1 & -1 & 1 & -1 \\ 1 & 1 & -1 & -1 \\ 1 & 1 & 1 & 1 \\ 1 & -1 & -1 & 1 \end{bmatrix}$$

Figure 8. An example of a multi-block unitary Hadamard matrix **Z**, whose blocks are four alphabetic Hadamard gates $\mathbf{H}_C$, $\mathbf{H}_A$, $\mathbf{H}_T$, $\mathbf{H}_G$.

As shown in Figure 9, this unitary matrix **Z** is the sum of 4 sparse matrices $\mathbf{z}_0$, $\mathbf{z}_1$, $\mathbf{z}_2$, $\mathbf{z}_3$ with a weight coefficient of 0.5, the set of which is closed under multiplication and defines a symmetric multiplication table of a special 4-dimensional algebra (the author has not found examples of the use of such an algebra in mathematical natural science, and will be grateful for any information about this algebra from readers).

$$\mathbf{Z} = 0.5\begin{bmatrix} 1,0,0,0 \\ 0,1,0,0 \\ 0,0,1,0 \\ 0,0,0,1 \end{bmatrix} + 0.5\begin{bmatrix} 0,-1,0,0 \\ 1,0,0,0 \\ 0,0,0,1 \\ 0,0,-1,0 \end{bmatrix} + 0.5\begin{bmatrix} 0,0,1,0 \\ 0,0,0,-1 \\ 1,0,0,0 \\ 0,-1,0,0 \end{bmatrix} + 0.5\begin{bmatrix} 0,0,0,-1 \\ 0,0,-1,0 \\ 0,1,0,0 \\ 1,0,0,0 \end{bmatrix} = 0.5(\mathbf{z}_0+\mathbf{z}_1+\mathbf{z}_2+\mathbf{z}_3)$$

© 2025 by the author(s). Distributed under a Creative Commons CC BY license.

Preprints.org (www.preprints.org) | NOT PEER-REVIEWED | Posted: 10 February 2026 doi:10.20944/preprints202512.0208.v2

•	z_0	z_1	z_2	z_3
z_0	z_0	z_1	z_2	z_3
z_1	z_1	$-z_0$	$-z_3$	z_2
z_2	z_2	$-z_3$	z_0	$-z_1$
z_3	z_3	z_2	$-z_1$	$-z_0$

1	1	1	1
1	-1	-1	1
1	-1	1	-1
1	1	-1	-1

Figure 9. Representation of the unitary Hadamard operator **Z** from Figure 8 as the sum of four sparse matrices z_0, z_1, z_2, z_3 with a weighting factor of 0.5. Bottom row: the symmetric multiplication table of these matrices (left) and the (4•4) Hadamard matrix with a similar arrangement of plus and minus signs (right for comparison).

The symmetric matrix multiplication table for z_0, z_1, z_2, and z_3 shown in Figure 9 has interesting properties. The alternating plus and minus signs in its rows and columns corresponds to a complete orthogonal system of Walsh functions and is analogous to the alternating signs in the Hadamard matrix shown next to this table. In light of this, the 4-dimensional algebra corresponding to such a multiplication table of basic elements can be called a genetic 4-dimensional Hadamard algebra. The symmetry of the matrix multiplication table for z_0, z_1, z_2, and z_3 indicates their commutativity.

3.1. Representations of Unitary Hamiltonian Quaternions Based on Four Genetic Unitary Hadamard Matrices

Let us now turn to the formation of multi-block unitary Hadamard matrices (based on the genetic Hadamard gates H_C, H_A, H_T, H_G), representing the "unitary" Hamiltonian quaternions and biquaternions, which are associated with many things in physics, robotics, artificial intelligence, etc., and to which thousands of works have been devoted in the 20th century alone [Gsponer, Hurni, 2008]. This attention to them is due to the fact that quaternions are closely related to the Pauli matrices, the theory of the electromagnetic field, the quantum-mechanical theory of chemical valence, the theory of spins, the rotation of bodies in three-dimensional space, etc. In particular, the operators describing the vibrational-rotational states of molecules have a quaternion structure [Lobodenko, 2009].

Figure 10 shows a block matrix **Q**, the blocks of which are the genetic gates H_G and H_A. It is a unitary Hadamard (4•4)-matrix (the coefficient of 0.5 ensures unitarity of **Q**).

$$\mathbf{Q} = 2^{-0.5} \begin{array}{|c|c|} \hline H_G & H_A \\ \hline -H_A & H_G \\ \hline \end{array} = 0.5 \begin{array}{|c|c|c|c|} \hline 1 & 1 & -1 & 1 \\ \hline -1 & 1 & 1 & 1 \\ \hline 1 & -1 & 1 & 1 \\ \hline -1 & -1 & -1 & 1 \\ \hline \end{array}$$

Figure 10. Unitary matrix representation **Q** of the Hamiltonian quaternion.

Let us show that this matrix **Q** is a matrix representation of a quaternion. Indeed, as shown in Figure 11, this matrix Q is the sum of four sparse matrices v_0, v_1, v_2, v_3: $\mathbf{Q} = 0.5(v_0 + v_1 + v_2 + v_3)$, where v_0 is the identity matrix. The set of these sparse matrices is closed under multiplication and determines their multiplication table, which coincides with the well-known multiplication table of the basic elements of the Hamiltonian quaternion algebra [Kantor, Solodovnikov, 1973]. This means that the matrix **Q** is a unitary matrix representation of the Hamiltonian quaternion $\mathbf{Q} = 0.5 + 0.5v_1 + 0.5v_2 + 0.5v_3$, где v_1, v_2, v_3 represent the imaginary units of this algebra. Quaternions and biquaternions that have unitary matrix representations can be called "unitary quaternions" and "unitary biquaternions" for brevity.

© 2025 by the author(s). Distributed under a Creative Commons CC BY license.

Preprints.org (www.preprints.org) | NOT PEER-REVIEWED | Posted: 10 February 2026 doi:10.20944/preprints202512.0208.v2

$$0.5\begin{bmatrix} 1, 1,-1,1 \\ -1, 1, 1,1 \\ 1,-1, 1,1 \\ -1,-1,-1,1 \end{bmatrix} = 0.5\begin{bmatrix} 1,0,0,0 \\ 0,1,0,0 \\ 0,0,1,0 \\ 0,0,0,1 \end{bmatrix} + 0.5\begin{bmatrix} 0,1, 0,0 \\ -1,0, 0,0 \\ 0,0, 0,1 \\ 0,0,-1,0 \end{bmatrix} + 0.5\begin{bmatrix} 0, 0,-1,0 \\ 0, 0, 0,1 \\ 1, 0, 0,0 \\ 0,-1, 0,0 \end{bmatrix} + 0.5\begin{bmatrix} 0, 0,0,1 \\ 0, 0,1,0 \\ 0,-1,0,0 \\ -1, 0,0,0 \end{bmatrix}$$

$$= 0.5(\mathbf{v}_0 + \mathbf{v}_1 + \mathbf{v}_2 + \mathbf{v}_3).$$

•	$\mathbf{v}_0$	$\mathbf{v}_1$	$\mathbf{v}_2$	$\mathbf{v}_3$
$\mathbf{v}_0$	$\mathbf{v}_0$	$\mathbf{v}_1$	$\mathbf{v}_2$	$\mathbf{v}_3$
$\mathbf{v}_1$	$\mathbf{v}_1$	$-\mathbf{v}_0$	$\mathbf{v}_3$	$-\mathbf{v}_2$
$\mathbf{v}_2$	$\mathbf{v}_2$	$-\mathbf{v}_3$	$-\mathbf{v}_0$	$\mathbf{v}_1$
$\mathbf{v}_3$	$\mathbf{v}_3$	$\mathbf{v}_2$	$-\mathbf{v}_1$	$-\mathbf{v}_0$

Figure 11. The unitary Hadamard matrix $\mathbf{Q} = 0.5(\mathbf{v}_0 + \mathbf{v}_1 + \mathbf{v}_2 + \mathbf{v}_3)$ as a sum of 4 sparse matrices. The multiplication table of this set of sparse matrices, closed under multiplication and corresponding to the multiplication table of the Hamiltonian quaternion algebra, is shown.

But the described unitary matrix representation of a quaternion through the formation of a block matrix, the blocks of which are the alphabetic Hadamard gates $\mathbf{H}_C$, $\mathbf{H}_A$, $\mathbf{H}_T$, $\mathbf{H}_G$, is not the only possible one. Figure 12 shows another version of such a matrix representation of a quaternion in the form of a unitary Hadamard (4•4)-matrix.

$$\mathbf{W} = 2^{-0.5}\begin{array}{|c|c|}\hline \mathbf{H}_G & -\mathbf{H}_A \\ \hline \mathbf{H}_A & \mathbf{H}_G \\ \hline \end{array} = 0.5\begin{array}{|cc|cc|}\hline 1 & 1 & 1 & -1 \\ -1 & 1 & -1 & -1 \\ \hline -1 & 1 & 1 & 1 \\ 1 & 1 & -1 & 1 \\ \hline \end{array}$$

Figure 12. An alternative version of the unitary matrix representation of the Hamiltonian quaternion in the form of a block matrix **W**.

Figure 13 shows that this matrix **W** is the sum of four sparse matrices $\mathbf{w}_0$, $\mathbf{w}_1$, $\mathbf{w}_2$, $\mathbf{w}_3$: $\mathbf{W} = 0.5(\mathbf{w}_0 + \mathbf{w}_1 + \mathbf{w}_2 + \mathbf{w}_3)$. The set of these sparse matrices is closed under multiplication and defines the same multiplication table of the Hamiltonian quaternion algebra as given above in Figure 11 for the case of a different quaternion representation in the form of a unitary Hadamard matrix.

$$\mathbf{W} = 0.5\begin{bmatrix} 1, 1, 1,-1 \\ -1, 1,-1,-1 \\ -1, 1, 1, 1 \\ 1, 1,-1, 1 \end{bmatrix} = 0.5\begin{bmatrix} 1,0,0,0 \\ 0,1,0,0 \\ 0,0,1,0 \\ 0,0,0,1 \end{bmatrix} + 0.5\begin{bmatrix} 0,1, 0,0 \\ -1,0, 0,0 \\ 0,0, 0,1 \\ 0,0,-1,0 \end{bmatrix} + 0.5\begin{bmatrix} 0,0,1, 0 \\ 0,0, 0,-1 \\ -1,0, 0, 0 \\ 0,1, 0, 0 \end{bmatrix} + 0.5\begin{bmatrix} 0,0, 0,-1 \\ 0,0,-1, 0 \\ 0,1, 0, 0 \\ 1, 0, 0, 0 \end{bmatrix}$$

$$= 0.5(\mathbf{w}_0 + \mathbf{w}_1 + \mathbf{w}_2 + \mathbf{w}_3).$$

•	$\mathbf{w}_0$	$\mathbf{w}_1$	$\mathbf{w}_2$	$\mathbf{w}_3$
$\mathbf{w}_0$	$\mathbf{w}_0$	$\mathbf{w}_1$	$\mathbf{w}_2$	$\mathbf{w}_3$
$\mathbf{w}_1$	$\mathbf{w}_1$	$-\mathbf{w}_0$	$\mathbf{w}_3$	$-\mathbf{w}_2$
$\mathbf{w}_2$	$\mathbf{w}_2$	$-\mathbf{w}_3$	$-\mathbf{w}_0$	$\mathbf{w}_1$
$\mathbf{w}_3$	$\mathbf{w}_3$	$\mathbf{w}_2$	$-\mathbf{w}_1$	$-\mathbf{w}_0$

1	1	1	1
1	-1	1	-1
1	-1	-1	1
1	1	-1	-1

Figure 13. The unitary Hadamard matrix $\mathbf{W} = 0.5(\mathbf{w}_0 + \mathbf{w}_1 + \mathbf{w}_2 + \mathbf{w}_3)$ as a sum of 4 sparse matrices. The bottom row gives the multiplication table of this set of sparse matrices, closed under multiplication. This table has the same arrangement of plus and minus signs as the Hadamard (4•4)-matrix shown to the right for comparison.

© 2025 by the author(s). Distributed under a Creative Commons CC BY license.

Preprints.org (www.preprints.org) | NOT PEER-REVIEWED | Posted: 10 February 2026 doi:10.20944/preprints202512.0208.v2

Let us note in passing that these two unitary matrix representations of the Hamiltonian quaternion **Q** and **W** (Figures 10 and 12) are not commutative and their commutator **K** is not equal to zero (4):

$$\mathbf{K} = \mathbf{Q} \bullet \mathbf{W} - \mathbf{W} \bullet \mathbf{Q} = [0, 0, -1, -1; 0, 0, -1, 1; 1, 1, 0, 0; 1, -1, 0, 0] \quad (4)$$

When raised to a power, a unitary quaternion forms cyclic unitary groups with period 6. An example of 6 members of one period of such a group $\mathbf{Q}^n$ is given in Figure 14.

$$\mathbf{Q}^1 = 0.5 \begin{bmatrix} 1, & 1, & -1, & 1 \\ -1, & 1, & 1, & 1 \\ 1, & -1, & 1, & 1 \\ -1, & -1, & -1, & 1 \end{bmatrix} ; \quad \mathbf{Q}^2 = 0.5 \begin{bmatrix} -1, & 1, & -1, & 1 \\ -1, & -1, & 1, & 1 \\ 1, & -1, & -1, & 1 \\ -1, & -1, & -1, & -1 \end{bmatrix} ; \quad \mathbf{Q}^3 = 0.5 \begin{bmatrix} -1, & 0, & 0, & 0 \\ 0, & -1, & 0, & 0 \\ 0, & 0, & -1, & 0 \\ 0, & 0, & 0, & -1 \end{bmatrix}$$

$$\mathbf{Q}^4 = 0.5 \begin{bmatrix} -1, & -1, & 1, & -1 \\ 1, & -1, & -1, & -1 \\ -1, & 1, & -1, & -1 \\ 1, & 1, & 1, & -1 \end{bmatrix} ; \quad \mathbf{Q}^5 = 0.5 \begin{bmatrix} 1, & -1, & 1, & -1 \\ 1, & 1, & -1, & -1 \\ -1, & 1, & 1, & -1 \\ 1, & 1, & 1, & 1 \end{bmatrix} ; \quad \mathbf{Q}^6 = 0.5 \begin{bmatrix} 1, & 0, & 0, & 0 \\ 0, & 1, & 0, & 0 \\ 0, & 0, & 1, & 0 \\ 0, & 0, & 0, & 1 \end{bmatrix}$$

Figure 14. Powers of the unitary Hamiltonian quaternion $\mathbf{Q}^n$ for n = 1, 2, 3, 4, 5, 6.

The members of the cyclic group of the unitary quaternion $\mathbf{Q}^n$ shown in Figure 14 are mutually consistent under the addition operation. Indeed, this cyclic group of unitary quaternions $\mathbf{Q}^n$ with period 6 has the following properties, which can be conveniently illustrated by arranging the sequence of matrix members of the group on a clock-shaped circle (Figure 15):

- 1) Unitary quaternions lying opposite on a circle are opposite in sign ($\mathbf{Q}^k = -\mathbf{Q}^{k+3}$) and when added give zero, that is, they are mutually complementary;

- 2) Each unitary quaternion on a circle is the sum of two adjacent unitary quaternions located on its sides, that is, $\mathbf{Q}^k = \mathbf{Q}^{k-1} + \mathbf{Q}^{k+2}$;

- 3) The sum of the unitary quaternions at the vertices of each of the two triangles of the "Star of David" is equal to zero, that is, $\mathbf{Q}_1 + \mathbf{Q}_3 + \mathbf{Q}_5 = \mathbf{Q}_2 + \mathbf{Q}_4 + \mathbf{Q}_6$ = the zero matrix.

These cyclic groups of unitary quaternions can be used to model biological systems as quantum-logical objects. One possible model application of this cyclic power group of unitary quaternions with period 6 concerns inherited color perception, the properties of which structurally correspond to Newton's 6-sector color circle shown in Figure 15. This figure also depicts all 6 members of one period of the cyclic group of the unitary quaternion $\mathbf{Q}^n$ from Figure 14 (i.e., $\mathbf{Q}^1$, $\mathbf{Q}^2$, $\mathbf{Q}^3$, $\mathbf{Q}^4$, $\mathbf{Q}^5$, $\mathbf{Q}^6$) as unitary matrix representations of these colors.

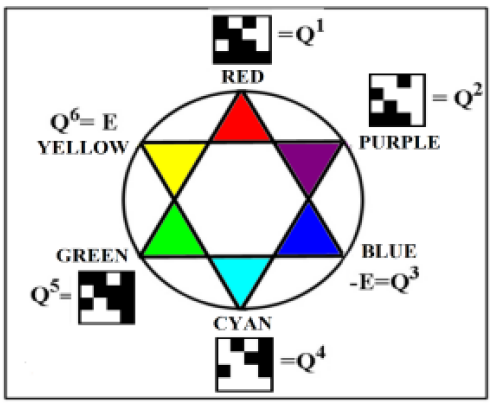

Figure 15. Newton's color circle from the psychophysics of color perception and the corresponding matrix members of the cyclic group of the unitary Hamiltonian quaternion $\mathbf{Q}^n$, whose period is 6. In each matrix, black

© 2025 by the author(s). Distributed under a Creative Commons CC BY license.

Preprints.org (www.preprints.org) | NOT PEER-REVIEWED | Posted: 10 February 2026 doi:10.20944/preprints202512.0208.v2

cells contain the numbers "+0.5" and white cells contain the numbers "-0.5." The symbol **E** denotes the identity matrix.

The listed properties of the cyclic group of Hamilton's unitary quaternion $\mathbf{Q}^n$ turn out to be identical to the phenomenological properties of inherited color perception, represented on Newton's six-sector color circle (Figure 15). This circle illustrates that color perception is based on three primary colors (red, blue, green) and three complementary colors (cyan, yellow, magenta), located at the vertices of two triangles of its "Star of David". On Newton's color circle, color perception is represented by the following well-known phenomenological properties, analogous to the just-mentioned structural-algebraic properties of the ensemble of members of the cyclic group of unitary quaternions $\mathbf{Q}^n$:

- 1) colors opposite each other on the color wheel are complementary and cancel each other out when superimposed;
- 2) each color on the color wheel is the sum of the two colors on its sides;
- 3) the three primary colors, like the three complementary colors at the vertices of the two triangles of the "Star of David," cancel each other out when superimposed.

The color mixing problem can now be formally solved in the quantum-logical language of the cyclic group of Hamiltonian unitary quaternions (constructed on the genetic alphabet of Hadamard unitary gates) if we assign to each of the 6 colors of the Newton circle a unitary quaternion **Q** to the corresponding power, as shown in Figure 15. For example, what color do you get if you mix 3 parts red, 2 parts yellow, and 5 parts blue? The answer is obtained by adding the corresponding unitary quaternions: $3\mathbf{Q}^1 + 2\mathbf{Q}^6 + 5\mathbf{Q}^3 = 3\mathbf{Q}^2$, i.e. 3 parts purple. In psychophysics, it is known that color is not a physical property of an object, but an inherited psychophysical reaction of a person to the light impact coming from the object, taking into account the general light environment. In modern literature, the features of color perception, like other features of sensory experience, are denoted by the term "qualia"; The topic of qualia is one of the most pressing and widely discussed topics in modern philosophy, which sees it as the key to understanding the nature of consciousness.

If we take a unitary quaternion to the fractional power 1/k, where k is a positive integer, and then raise it to integer powers n, then, using the resulting cyclic sequence of unitary quaternions $\mathbf{Q}^{n/k}$, we can, by choosing the appropriate value of k, divide Newton's color circle into any desired number of parts—for example, into 80, and not just into 6 as in Newton's circle. Moreover, each part of the circle in this division is associated with its own unitary quaternion to the appropriate power. Based on the classical color wheel in Figure 15 and the mapping of each base color to a unitary quaternion to the corresponding power, we can use the mathematics of unitary quaternions to calculate which specific color hue, for example, out of 80 hues, corresponds to a unitary quaternion to a specific power. In other words, a regular sequence of unitary quaternions in fractional powers can be compared to a regular sequence of the same number of color hues, each of which receives its own mathematical identification, expressed by a unitary quaternion to the appropriate power. Thus, we obtain a regular "unitary-quaternion palette" of color hues, arbitrarily detailed. The sequence of unitary quaternions $\mathbf{Q}^{n/k}$ (where n = 1, 2, 3, …) under consideration is endowed with the following regularities:

$$\mathbf{Q}^{n/k} = \mathbf{Q}^{n/k\ +6};\ \mathbf{Q}^{n/k} = \mathbf{Q}^{n/k-1} + \mathbf{Q}^{n/k+1};\ \mathbf{Q}^{n/k} = -\mathbf{Q}^{n/k+3} \quad (5)$$

The founder of the wave theory of quantum mechanics, E. Schrödinger, conducted fundamental research in the field of color metrics and the theory of color perception between 1920 and 1926, based on the idea that understanding the laws of human sensory perception of the world is important for all of physics; his key idea was that the space of color perception has a non-Euclidean nature [Schrödinger, 1971; Niall, 2017]. In passing, we note the existence of a certain analogy between a circle divided into arbitrarily small fragments by an ordered sequence of such power unitary quaternions and ancient ideas about the cycle of rebirths (for example, samsara or the wheel of samsara is one of the central concepts in ancient Indian philosophy).

© 2025 by the author(s). Distributed under a Creative Commons CC BY license.

Preprints.org (www.preprints.org) | NOT PEER-REVIEWED | Posted: 10 February 2026 doi:10.20944/preprints202512.0208.v2

This comparison of an ordered sequence of unitary quaternions with a corresponding ordered sequence of color hues is useful, for example, in connection with the well-known psychophysical Lüscher color test [Lüscher, 1971; Dragunsky, 2001; Spasennikov, 2019; Tsyganok, 2007]. It is used, in particular, in ergonomics to assess a worker's psychophysiological state, their stress tolerance, activity level, communication skills, optimal career guidance, etc. During the Lüscher test, the subject is presented with a set of cards of different colors (there may be several dozens of them), which the subject must arrange in a sequence starting with the most pleasant color hues to the most unpleasant. Based on the resulting color sequence, the specialist draws the desired conclusion about the subject's psychophysiological state. Taking into account our above-described data, we can now represent the color sequence obtained in the test as a sequence of corresponding unitary Hamiltonian quaternions, with its mathematical analysis carried out for a more in-depth characterization of the psychophysiological state of the subject, associated with his genetic quantum-logical characteristics.

Cyclic groups of unitary quaternions can also be used for quantum logic modeling, for example, of innate algorithmic movements of limbs in human and animal locomotion; the formation of the three-dimensional structure of proteins based on relative rotations of adjacent segments of the protein molecule (protein folding); and so on. The possible leading role of Hamiltonian quaternion operators in protein folding (with their special connection to rotations in three-dimensional physical space) has already been previously suggested in [Carlevaro, Irastorz, Vericat, 2016], along with an attempt (unrelated to quantum logic, quantum information science, and unitary operators) to treat nucleotide and amino acid sequences as sequences of quaternions.

3.2. Representations of Unitary Biquaternions Based on Genetic Unitary Hadamard Matrices

Figure 16 shows an example of an (8•8)-matrix **B**, whose (2•2)-blocks are alphabetic genetic Hadamard's gates. It is a unitary Hadamard matrix representing a biquaternion. Its unitarity follows from its satisfaction of the unitarity criterion: $\mathbf{B} \bullet \mathbf{B}^{\mathrm{T}} = \mathbf{E}$, where $\mathbf{B}^{\mathrm{T}}$ is the transpose of **B** and **E** is the identity matrix of order eight.

$$\mathbf{B} = 0.5 \begin{vmatrix} H_G & H_A & -H_G & -H_A \\ -H_A & H_G & H_A & -H_G \\ H_G & H_A & H_G & H_A \\ -H_A & H_G & -H_A & H_G \end{vmatrix} = 2^{-1.5} \begin{vmatrix} 1 & 1 & -1 & 1 & -1 & -1 & 1 & -1 \\ -1 & 1 & 1 & 1 & 1 & -1 & -1 & -1 \\ 1 & -1 & 1 & 1 & -1 & 1 & -1 & -1 \\ -1 & -1 & -1 & 1 & 1 & 1 & 1 & -1 \\ 1 & 1 & -1 & 1 & 1 & 1 & -1 & 1 \\ -1 & 1 & 1 & 1 & -1 & 1 & 1 & 1 \\ 1 & -1 & 1 & 1 & 1 & -1 & 1 & 1 \\ -1 & -1 & -1 & 1 & -1 & -1 & -1 & 1 \end{vmatrix}$$

Figure 16. The block matrix **B** of the eighth order is a unitary Hadamard matrix.

Let us show that it serves as a matrix representation of a biquaternion. Indeed, matrix **B** is the sum of 8 sparse matrices, the set of which is closed under multiplication and defines the multiplication table known in biquaternion algebra and shown in Figure 17.

© 2025 by the author(s). Distributed under a Creative Commons CC BY license.

Preprints.org (www.preprints.org) | NOT PEER-REVIEWED | Posted: 10 February 2026 doi:10.20944/preprints202512.0208.v2

$$\mathbf{B} = 2^{-1.5}\begin{bmatrix}1&0&0&0&0&0&0&0\\0&1&0&0&0&0&0&0\\0&0&1&0&0&0&0&0\\0&0&0&1&0&0&0&0\\0&0&0&0&1&0&0&0\\0&0&0&0&0&1&0&0\\0&0&0&0&0&0&1&0\\0&0&0&0&0&0&0&1\end{bmatrix} + 2^{-1.5}\begin{bmatrix}0&1&0&0&0&0&0&0\\-1&0&0&0&0&0&0&0\\0&0&0&1&0&0&0&0\\0&0&-1&0&0&0&0&0\\0&0&0&0&0&1&0&0\\0&0&0&0&0&0&-1&0\\0&0&0&0&0&0&0&1\\0&0&0&0&0&0&-1&0\end{bmatrix} + 2^{-1.5}\begin{bmatrix}0&0&-1&0&0&0&0&0\\0&0&0&1&0&0&0&0\\1&0&0&0&0&0&0&0\\0&-1&0&0&0&0&0&0\\0&0&0&0&0&0&-1&0\\0&0&0&0&0&0&0&1\\0&0&0&0&1&0&0&0\\0&0&0&0&0&-1&0&0\end{bmatrix} +$$

$$+ 2^{-1.5}\begin{bmatrix}0&0&0&1&0&0&0&0\\0&0&1&0&0&0&0&0\\0&-1&0&0&0&0&0&0\\-1&0&0&0&0&0&0&0\\0&0&0&0&0&0&0&1\\0&0&0&0&0&0&1&0\\0&0&0&0&0&-1&0&0\\0&0&0&0&-1&0&0&0\end{bmatrix} + 2^{-1.5}\begin{bmatrix}0&0&0&0&-1&0&0&0\\0&0&0&0&0&-1&0&0\\0&0&0&0&0&0&-1&0\\0&0&0&0&0&0&0&-1\\1&0&0&0&0&0&0&0\\0&1&0&0&0&0&0&0\\0&0&1&0&0&0&0&0\\0&0&0&1&0&0&0&0\end{bmatrix} + 2^{-1.5}\begin{bmatrix}0&0&0&0&-1&0&0&0\\0&0&0&0&1&0&0&0\\0&0&0&0&0&0&-1&0\\0&0&0&0&0&1&0&0\\0&1&0&0&0&0&0&0\\-1&0&0&0&0&0&0&0\\0&0&0&1&0&0&0&0\\0&0&-1&0&0&0&0&0\end{bmatrix} +$$

$$+ 2^{-1.5}\begin{bmatrix}0&0&0&0&0&1&0&0\\0&0&0&0&0&0&-1&0\\0&0&0&0&-1&0&0&0\\0&0&0&0&1&0&0&0\\0&0&-1&0&0&0&0&0\\0&0&1&0&0&0&0&0\\1&0&0&0&0&0&0&0\\0&-1&0&0&0&0&0&0\end{bmatrix} + 2^{-1.5}\begin{bmatrix}0&0&0&0&0&0&-1&0\\0&0&0&0&0&0&0&-1\\0&0&0&0&0&1&0&0\\0&0&0&0&1&0&0&0\\0&0&0&1&0&0&0&0\\0&0&1&0&0&0&0&0\\0&-1&0&0&0&0&0&0\\-1&0&0&0&0&0&0&0\end{bmatrix}$$

•	b_0	b_1	b_2	b_3	b_4	b_5	b_6	b_7
b_0	b_0	b_1	b_2	b_3	b_4	b_5	b_6	b_7
b_1	b_1	$-b_0$	b_3	$-b_2$	b_5	$-b_4$	b_7	$-b_6$
b_2	b_2	$-b_3$	$-b_0$	b_1	b_6	$-b_7$	$-b_4$	b_5
b_3	b_3	b_2	$-b_1$	$-b_0$	b_7	b_6	$-b_5$	$-b_4$
b_4	b_4	b_5	b_6	b_7	$-b_0$	$-b_1$	$-b_2$	$-b_3$
b_5	b_5	$-b_4$	b_7	$-b_6$	$-b_1$	b_0	$-b_3$	b_2
b_6	b_6	$-b_7$	$-b_4$	b_5	$-b_2$	b_3	b_0	$-b_1$
b_7	b_7	b_6	$-b_5$	$-b_4$	$-b_3$	$-b_2$	b_1	b_0

Figure 17. Decomposition of the unitary (8•8)-matrix **B** from Figure 16 into a sum of 8 sparse matrices ($\mathbf{B} = 2^{-1.5}(\mathbf{b}_0+\mathbf{b}_1+\mathbf{b}_2+\mathbf{b}_3+\mathbf{b}_4+\mathbf{b}_5+\mathbf{b}_6+\mathbf{b}_7)$ whose set is closed under multiplication and defines the multiplication table shown below on the right. Here $\mathbf{b}_0$ is the identity matrix.

Thus, the unitary matrix **B** is a matrix representation of the biquaternion $\mathbf{B} = 2^{-1.5}(\mathbf{b}_0+\mathbf{b}_1+\mathbf{b}_2+\mathbf{b}_3+\mathbf{b}_4+\mathbf{b}_5+\mathbf{b}_6+\mathbf{b}_7)$, which can be called a unitary biquaternion. Raising this unitary biquaternion **B** to integer powers generates a cyclic group of unitary transformations with period 24 and a number of regular relations among group members (including the opposite-sign members, separated by 12 powers) as it is shown in (6):

$$\mathbf{B}^n = \mathbf{B}^{n+24},\ \mathbf{B}^n = -\mathbf{B}^{n+12},\ \mathbf{B}^n = \mathbf{B}^{n-4} + \mathbf{B}^{n+4},\ \mathbf{B}^n = -(\mathbf{B}^{n-8} + \mathbf{B}^{n+8}),\ \mathbf{B}^n = 2^{-0.5}(\mathbf{B}^{n-3} + \mathbf{B}^{n+3}) \quad (6)$$

The quantum-logical properties of this cyclic unitary group allow it to be used to model the features of 24-hour biorhythms (circadian rhythms), especially since biquaternions are traditionally used in physics to model spatiotemporal relationships. It has been known since ancient times that various physiological subsystems of our body undergo coordinated phases of activity and passivity throughout the day, which, according to ancient and modern medicine, explains the division of the human day into 24 hours [Wright, 2002]. Time is called the "fundamental factor of life," felt by all organisms at all times [ibid.]. The biorhythmic organization of inherited processes is distributed throughout the body of organisms of the most diverse species, including those without a nervous system. The biological clock, counting down minutes, months, and years, ensures the coordinated functioning of body parts according to a specific plan. It is responsible for the aging process and death, and its disruptions are associated with cancer, Parkinson's disease, and other diseases.

The cyclic group of the unitary biquaternion **B**, obtained by raising it to integer powers and having a period of 24 (that is, a sequence of powers 1, 2, 3, …, 24 in one period of this group of unitary operators $\mathbf{B}^n$), is in our quantum-logical approach an analogue of the 24-hour clock in Figure 18 and, accordingly, a model of the circadian 24-hour biorhythms (this is clearly demonstrated by arranging the sequence of 24 members of one period of this cyclic group $\mathbf{B}^n$ on the clock dial divided into 24 parts as shown in Figure 18). The unitary biquaternions $\mathbf{B}^n$ and $\mathbf{B}^{n+12}$, opposite each other on such a

© 2025 by the author(s). Distributed under a Creative Commons CC BY license.

Preprints.org (www.preprints.org) | NOT PEER-REVIEWED | Posted: 10 February 2026 doi:10.20944/preprints202512.0208.v2

clock face, differ only in their opposite sign ($\mathbf{B}^n = -\mathbf{B}^{n+12}$), similar to the oppositions of hours of day and night times.

Figure 18. A 24-hour clock dial, divided into 12-hour day and night halves. The numbers on the clock correspond to the exponents 1, 2, 3, …, 23, 24 in the set of 24 members of a single period of the cyclic group of unitary biquaternions $\mathbf{B}^n$, obtained by raising the biquaternion **B** from Figures 16 and 17 to integer powers.

Note that, similar to the above-described raising of a unitary quaternion to fractional powers, one can, by raising the unitary biquaternion B to fractional powers, partition the model 24-hour clock into smaller divisions, for example, 1440 minutes or 86400 seconds, as well as into larger divisions, for example, eight 3-hour divisions. This transition to sequences of smaller time intervals is useful for the model-by-cycle analysis of the corresponding relatively fast biological processes in the quantum-logical language of unitary biquaternions. This theme of cyclic changes of a unitary biquaternion raised to a power is related to the diagrams of the ancient Chinese "Book of Cyclical Changes" ("I Ching"), which had a strong influence on the oriental medicine of China, Japan, Korea, and elsewhere and formed the basis of circular Chinese calendars in connection with the concept of cyclic time and universal patterns. In particular, with the help of ensembles of such dials (Figure 18), each of which is cyclically divided by exponential cyclic sequences of unitary biquaternions into the corresponding number of parts, it is possible to model a variety of complex rhythms, taking into account the well-known rhythm-logical theory of I. Schillinger [Schillinger, 1958]. A consideration of the interesting topic of the unitary quaternion $\mathbf{Q}^{f(t)}$ and the unitary biquaternion $\mathbf{B}^{f(t)}$ in powers of an arbitrary cyclic function f(t) is beyond the scope of this article.

Overall, the quantum-logical approach developed by the author, which includes, in particular, the aforementioned unitary quaternions and biquaternions, allows for the modeling of a wide variety of cyclical bioprocesses and biostructures. These include, for example, the replication of DNA strands based on the cyclical sequential reading of their nucleotides, which sometimes occurs at astonishing speeds. For example, the cyclical process of step-by-step replication of the DNA nucleotide sequence in the bacterium Escherichia coli occurs at a rate of over 1000 nucleotides per second, that is, more than a hundred times faster than the fastest machine gun [Bank, 2022]. Somatic cells of the body divide cyclically (cell mitosis), which is accompanied by a cyclical change in the stages of cell division. Proteins with the characteristic name "cyclins" play an important role in this process; their concentration in the cell changes cyclically. These interconnected cyclical phenomena are closely intertwined with the topic of internal biological clocks, the study of the molecular cyclical basis of which was awarded the Nobel Prize in 2017 for showing that all multicellular organisms, including humans, use a similar cyclical molecular mechanism of internal clocks to control circadian biorhythms [Press release, 2017].

Of interest for quantum logic modeling based on genetic alphabets of Hadamard gates and associated cyclic groups of unitary operators is the structure of nucleosomes as an octameric rod consisting of four types of histone proteins with complementarity relationships between histones. The octameric structure of nucleosomes plays a central role in DNA packaging at all levels. Also of

© 2025 by the author(s). Distributed under a Creative Commons CC BY license.

Preprints.org (www.preprints.org) | NOT PEER-REVIEWED | Posted: 10 February 2026 doi:10.20944/preprints202512.0208.v2

interest is the cyclic structure of telomeres, which are the tips of DNA molecules. Each cycle of cell division is typically accompanied by shortening of its telomeres (the terminal regions of DNA), which is considered by many authors to be a biological clock mechanism and an indicator of aging. The topic of telomeres is linked to oncology research, as cancer cells often bypass the mechanism that limits cell division [Xu, Cheng, Zhao, et al, 2021]. Telomeres in humans and vertebrates are characterized by thousands of cyclic repeats of the 6-nucleotide sequence TTAGGG, which can be viewed, in particular, from the perspective of a cyclic power group of unitary quaternions with a period of 6. Cyclomer multiblock forms of living bodies (mollusk shells, etc.) also represent a vast area for the described quantum logic modeling using cyclic groups of unitary operators. A series of papers [Fimmel, Michel, Pirot, et al, 2019; Fimmel, Starman, Strüngmann, 2020; Fimmel, Michel, Pirot, et al, 2020, and others] are devoted to the substantive topic of cyclic shifts in genetic code sequences. Research into inherited ensembles of cyclic bioprocesses is important, among other things, for the intensification of crop and livestock production in connection with the current tasks of developing agriculture and agricultural engineering [Chernoyvanov, Petukhov, Rajan, Tolokonnikov, 2025].

It should be noted that artistic creativity has always involved the use of cyclical and hyper-cyclical constructs (music, poetry, architecture, etc.). The famous book “The Glass Bead Game” by Nobel laureate in literature Heinrich Hesse is dedicated to a game whose goal is to find a deep structural-mathematical connection between objects from different fields of science and art [Hesse, 2007]. Essentially, the “Glass Bead Game” is the art of composing a metatext, a synthesis of all branches of art into a single, universal art. In our opinion, the genetic texts of DNA, with their hidden patterns and their interaction with the formalisms of quantum logic, are the metatexts upon which biological texts and cyclical constructs of various kinds are built, including those of human mathematical and artistic creativity.

3.3. Projection Operators Based on Genetic Unitary Hadamard Matrices

In quantum logic, all operators must be unitary (invertible) except the measurement operator. Quantum logic is based on the algebra of projections in Hilbert space, and the measurement operator is related to the concept of a projection operator **P** (projector), the criterion for which is the condition $\mathbf{P}^2 = \mathbf{P}$. Is it possible to construct such an irreversible projection operator from alphabetic Hadamard gates $\mathbf{H}_C$, $\mathbf{H}_A$, $\mathbf{H}_T$, $\mathbf{H}_G$? It turns out that it is possible, and Figure 19 provides an example of such a matrix projector.

$$\mathbf{P} = 2^{-0.5} \bullet \begin{array}{|c|c|} \hline \mathbf{H}_C & -\mathbf{H}_A \\ \hline -\mathbf{H}_A & \mathbf{H}_C \\ \hline \end{array} = 2^{-1} \bullet \begin{array}{|c|} \hline 1, -1, 1, -1 \\ 1, 1, -1, -1 \\ 1, -1, 1, -1 \\ -1, -1, 1, 1 \\ \hline \end{array}$$

Figure 19. An example of a matrix projector **P** based on alphabetic Hadamard matrices.

The matrix operator P shown in Figure 19 has a zero determinant, i.e., it is an irreversible operator. It satisfies the projector criterion: $\mathbf{P}^2 = \mathbf{P}$. Thus, it satisfies the above-mentioned requirements for a measurement operator in quantum logic. Moreover, it is related to the system of Rademacher orthogonal functions, which is widely known in mathematics and its applications: the rows of the matrix (shown in Figure 19 on the right) represent a set of Rademacher functions taking values ±1. In the general case, the Rademacher functions are defined by the expression $rad_n(x) = \text{sign}(\sin(2^n \pi x))$ on the interval [0, 1]. Graphically, each Rademacher function is a rectangular wave (meander) with a frequency of 2^{n-1}. The Rademacher function system is a classical object of orthogonal series theory and probability theory, with numerous applications both within these fields and in a number of related fields, primarily in the geometric theory of Banach spaces, operator theory, harmonic analysis, and mathematical statistics [Astashkin, 2017]. Specifically, the Rademacher function system is used in

© 2025 by the author(s). Distributed under a Creative Commons CC BY license.

Preprints.org (www.preprints.org) | NOT PEER-REVIEWED | Posted: 10 February 2026 doi:10.20944/preprints202512.0208.v2

wavelet theory and the theory of random series, with deep connections to fundamental concepts of convergence, random processes, and harmonic analysis. This article presents a new realization of Rademacher functions as rows in genetic Rademacher matrices as possible measurement operators in the quantum logic of biosystems, or more precisely, in the described new bioinformatics system based on genetic alphabets of unitary Hadamard operators and quantum logic formalisms.

This "Rademacher projector" **P** in Figure 19 is conjugate to the 4-dimensional algebra of hypercomplex numbers known as split-quaternions of Cockle. Indeed, this matrix projector **P**, as shown in Figure 20, is the sum of 4 sparse unitary matrices $\mathbf{p}_0$, $\mathbf{p}_1$, $\mathbf{p}_2$, $\mathbf{p}_3$ (weighted 0.5), the set of which is closed under multiplication and defines their multiplication table, which coincides with the multiplication table of the basic elements of the Cockle split-quaternion algebra. Split-quaternions have long been used in the conformal Poincaré disk model of Lobachevsky hyperbolic geometry to describe hyperbolic motions (Figure 20 additionally shows the symbol of this Poincaré disk model).

$$\mathbf{P} = 2^{-0.5}\begin{bmatrix} 1,0,0,0 \\ 0,1,0,0 \\ 0,0,1,0 \\ 0,0,0,1 \end{bmatrix} + 2^{-0.5}\begin{bmatrix} 0,-1,0,0 \\ 1,0,0,0 \\ 0,0,0,-1 \\ 0,0,1,0 \end{bmatrix} + 2^{-0.5}\begin{bmatrix} 0,0,1,0 \\ 0,0,0,-1 \\ 1,0,0,0 \\ 0,-1,0,0 \end{bmatrix} + 2^{-0.5}\begin{bmatrix} 0,0,0,-1 \\ 0,0,-1,0 \\ 0,-1,0,0 \\ -1,0,0,0 \end{bmatrix} = 2^{-0.5}(\mathbf{p}_0+\mathbf{p}_1+\mathbf{p}_2+\mathbf{p}_3)$$

•	$\mathbf{p}_0$	$\mathbf{p}_1$	$\mathbf{p}_2$	$\mathbf{p}_3$
$\mathbf{p}_0$	$\mathbf{p}_0$	$\mathbf{p}_1$	$\mathbf{p}_2$	$\mathbf{p}_3$
$\mathbf{p}_1$	$\mathbf{p}_1$	$-\mathbf{p}_0$	$-\mathbf{p}_3$	$\mathbf{p}_2$
$\mathbf{p}_2$	$\mathbf{p}_2$	$\mathbf{p}_3$	$\mathbf{p}_0$	$\mathbf{p}_1$
$\mathbf{p}_3$	$\mathbf{p}_3$	$-\mathbf{p}_2$	$-\mathbf{p}_1$	$\mathbf{p}_0$

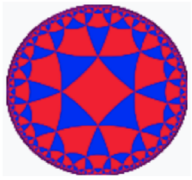

Figure 20. Decomposition of the Rademacher matrix projector **P** (Figure 19) into a sum of 4 sparse unitary matrices $\mathbf{p}_0+\mathbf{p}_1+\mathbf{p}_2+\mathbf{p}_3$ (taken with a factor of 0.5), the set of which is closed under multiplication and corresponds to the shown multiplication table of the algebra of 4-dimensional split-quaternions of Cockle. The symbol for the Poincaré disk model is also shown.

The identification of this algebraic-logical connection between the genetic coding system and hyperbolic geometry through the Rademacher projector allows seeing a genetic quantum-logical basis in the known conjugations of the following physiological phenomena with this geometry:

-1) the hyperbolic geometry of the space of visual perception [Luneburg, 1950; Kienle, 1964];

-2) the spatio-temporal organization of locomotion in humans and animals [Smolyaninov, 2000];

-3) the morphogenetic phenomena of phyllotaxis [Bodnar, 1992, 1994].

These authors did not suppose a connection between the bio-phenomena they discovered and the quantum-logical structures of molecular genetic coding.

Shown in Figure 19, the projector matrix **P** with rows in the form of Rademacher functions has been repeatedly encountered earlier in the author's publications on matrix genetics in connection with the algebraic description of the symmetric features of the genetic coding system associated with Rumer's rule on 32 strong and 32 weak roots in 64 genetic triplets (see, for example, the books [Petoukhov, 2008; Petoukhov, He, 2010, 2023]. This "Rademacher matrix" has a cross-shaped character: the quadrants along each of its two diagonals are identical. This is associated with the fact that many genetically inherited physiological systems are structured precisely in a cross-shaped manner. Thus, the conjugation of the hemispheres of the brain with the halves of the body is cross-shaped as weel-known: the left hemisphere serves the right half of the body, and the right hemisphere serves the left half. The optic nerve pathways from the two eyes are structured in a cross-shaped manner: they transmit information about the right half of the visual field to the left hemisphere of the brain, and information about the left half of the visual field to the right hemisphere. The same is true for the auditory system.

© 2025 by the author(s). Distributed under a Creative Commons CC BY license.

Preprints.org (www.preprints.org) | NOT PEER-REVIEWED | Posted: 10 February 2026 doi:10.20944/preprints202512.0208.v2

4. A Related Alphabet of Four Non-Unitary Operators for Bioinformatics of Inheritance in Open Quantum-Like Biosystems

The previous sections presented elements of the theory and applications of a bioinformation system based on the genetic alphabet of four Hadamard unitary operators. Accordingly, this system can be tentatively termed a "unitary bioinformation system," useful primarily for the above-described modeling of biological inheritance in a wide class of algorithmic cyclic and biorhythmic ensembles. In quantum mechanics, unitary operators describe the evolution of closed quantum systems.

But biology also knows the inheritance of structures that cannot, in principle, be described by this unitary operators bioinformatics of closed quantum systems and which should therefore be classified as bioinformatics of open (non-closed) quantum-like systems. This applies, for example, to the abundance of helical and helical structures at all levels of living body organization, often growing in stages during ontogenesis. Spirals are present in the heart, blood vessels, bones, nerves, cochlea, tendons and ligaments, alpha helices of proteins, collagen, flagella and cilia of the locomotor apparatus of bacteria and many protists, mollusk shells, animal horns, the cellular organization of the embryo (zygote), and so on. Due to the helicity of a huge number of inherited biological configurations, all fluid flows in the body—blood, lymph, urine—are helical. It is not without reason that Goethe called spirals "symbols of life" and a book with the revealing title "The Curves of Life" is dedicated to them [Cook, 1914]. Biological spirals can serve as bioantennas for the emission and reception of circularly polarized electromagnetic waves, forming highly efficient bioantenna arrays that determine communication and other functional features in many organisms; this is systematically examined with many biological examples in publications on the doctrine of energy-information evolution based on bioantenna arrays [Petoukhov, 2023; Petoukhov, 2022; Petoukhov, He, 2023].

Data on biological spirals are used in the bionics of spiral structures [Petoukhov, Svirin, Khazina, 2015; Petoukhov, He, 2023]. For example, spiral and fractal-spiral antennas are widely used in communications technology due to the generation of circularly polarized electromagnetic waves, which has many useful applications and is related to the topic of inherited chirality of biological structures and bioantenna arrays. Characteristically, inherited biological spirals often obey the known laws of phyllotaxis, which relate them to the Fibonacci numbers from the recurrent sequence $F_{n+2} = F_n + F_{n+1}$, starting with $F_0 = 0$, $F_1 = 1$ (Table 2). The study of spiral phyllotaxis and the features of its modular (block) structure has been conducted worldwide for about a century and a half, constituting one of the most famous sections of mathematical biology, to which many hundreds of publications are devoted and a review of which is available in the book [Jean, 1994; Jean, 2019].

Table 2. The initial fragment of the Fibonacci sequence $F_{n+2} = F_n + F_{n+1}$.

n	0	1	2	3	4	5	6	7	8	9	10	11	12	…
$\mathbf{F_n}$	0	1	1	2	3	5	8	13	21	34	55	89	144	…

Many spiral configurations of growing living bodies, for example, phyllotactic biospirals, consist of algorithmically repeating module forms, which is reminiscent of the ancient principle "like begets like", represented in the organization of the double helix of DNA, etc. [Petoukhov, 2023]. Such an algorithmic cyclic structure of biological bodies of plants, mollusk shells and many other types of organisms is accompanied by the implementation of similarity biosymmetries of A.V. Shubnikov and their generalizations in the form of conformal-geometric (locally-like or Möbius) biosymmetries [Petoukhov, 1989; Petoukhov, He, 2023]. The fact of inheritance of families of ordered biological spirals at all levels of the organization of living things gives rise to suspicion of the existence in living nature of another operator bioinformation system based on an algebraic-operator alphabet, suitable

© 2025 by the author(s). Distributed under a Creative Commons CC BY license.

Preprints.org (www.preprints.org) | NOT PEER-REVIEWED | Posted: 10 February 2026 doi:10.20944/preprints202512.0208.v2

for encoding and inheritance of spiral and helical structures, including phyllotaxis. Operators of such alphabetic bioinformatics should allow modeling of modular reproduction of helical configurations, including those associated with Fibonacci numbers.

Let's begin by describing such a "spiral" bioinformation system based on a genetic alphabet of four matrix operators, closely related to the above-described genetic alphabet of four unitary Hadamard matrices: both of these alphabets consist of related sets of four matrices that are trivial algorithmic modifications of each other. This alphabetic algebraic relationship allows both bioinformatics systems to function in a coordinated manner.

Multichannel Hadamard-transform spectrometers are known in technology, employing the principle of band or chain masks, reminiscent of the principle of genetic texts in heredity molecules [Tolmachev, 1976; Decker, Harwitt, 1976]. This Hadamard-matrix-based spectroscopy utilizes an algorithmic replacement of the element "-1" in the Hadamard matrices by the element "0". Let us used similar replacement in the considered alphabetic matrices.

Let's return to Table 1, in which the distribution of binary-opposition molecular features in the 4-nucleotide DNA alphabet is presented based on the binary numerical oppositions +1 and -1, revealing a connection with the Hadamard matrix alphabet. However, the same distribution of binary-opposition features in the nucleotide DNA alphabet can be represented based on the binary elements 1 and 0 by replacement of the element "-1" with the element "0" in Table 1. The result of this algorithmic substitution is presented in Table 3.

Table 3. Representation of a distribution of binary molecular features in the DNA alphabet of 4 nucleotides G, A, T, C with binary oppositions designated by the symbols +1 and 0. The fourth row of the table represents the presence of benzene rings in the molecules of all four nucleotides by using the symbol +1.

Molecular traits and their symbols	G	A	T	C
Pyrimidines +1, purines 0	0	0	+1	+1
Amino-nucleotides +1, keto-nucleotides 0	0	+1	0	+1
Complementarity with 3 or 2 hydrogen bonds: +1, 0	+1	0	0	+1
The presence of benzene rings +1	+1	+1	+1	+1

The right-hand side of this phenomenological Table 3 contains a matrix, all four quadrants of which have significant algebraic significance. We will designate the four second-order matrices in these quadrants as $\mathbf{D}_C$, $\mathbf{D}_A$, $\mathbf{D}_T$, $\mathbf{D}_G$ (in some analogy with the above-discussed alphabetic unitary matrices $\mathbf{H}_C$, $\mathbf{H}_A$, $\mathbf{H}_T$, $\mathbf{H}_G$). The lower right quadrant $\mathbf{D}_G = [0, 1; 1, 1]$ is the well-known Fibonacci matrix **F**, raising which to integer powers n generates a family of matrices, all elements of which are Fibonacci numbers $\mathbf{F}_n$ (Table 2), represented in the biological laws of spiral phyllotaxis (Figure 21).

$$\mathbf{F} = \begin{bmatrix} 0, 1 \\ 1, 1 \end{bmatrix}; \quad \mathbf{F}^2 = \begin{bmatrix} 1, 1 \\ 1, 2 \end{bmatrix}; \quad \mathbf{F}^n = \begin{bmatrix} F_{n-1}, F_n \\ F_n, F_{n+1} \end{bmatrix}$$

Figure 21. Fibonacci matrix $\mathbf{F} = \mathbf{D}_G$ and its powers.

In two quadrants along the second diagonal of the (4•4)-matrix in Table 3 are the (2•2)-matrices $\mathbf{D}_A = [1, 1; 0, 1]$ and $\mathbf{D}_T = [1, 0; 1, 1]$. They are matrix representations of hypercomplex dual numbers that underlie the screw calculus, which generalizes vector calculus and is associated with the names of W. Clifford, E. Study, A.P. Kotelnikov, and others [Dimentberg, 1965]. The screw calculus gives a compact description of the screw motion (rotation + translational displacement along the rotation axis) of rigid bodies in our physical three-dimensional space. The screw calculus is associated with the theory of electromagnetic waves and the helicity of photons; it has many applications in robotics, manipulator control, imitation learning, computer vision, computer graphics, information storage and processing (including quantum informatics), antenna technology, holography based on the

© 2025 by the author(s). Distributed under a Creative Commons CC BY license.

Preprints.org (www.preprints.org) | NOT PEER-REVIEWED | Posted: 10 February 2026 doi:10.20944/preprints202512.0208.v2

recording of a helical wavefront (in connection with optical vortices), etc. Dual numbers are also used in machine learning in connection with automatic differentiation, which is one of the key technologies in modern neural networks [Baydin, et al., 2018]. A dual number is a hypercomplex number of the form $a + \varepsilon b$, where a and b are real numbers, and ε is the dual imaginary unit or abstract element whose square is zero ($\varepsilon^2 = 0$), but is not itself equal to zero [Yaglom, 1963; Kisil, 2007]. Any dual number is uniquely determined by a pair of numbers a and b, where a is called the real part of the dual number, and b is its imaginary part. The set of all dual numbers forms a two-dimensional commutative associative algebra with unity under the multiplicative operation over the field of real numbers. Figure 26 shows the matrix representation of the dual number in the form of the mentioned (2•2)-matrices $\mathbf{D}_A$ and $\mathbf{D}_T$, each of which is the sum of two sparse matrices: the first of which is the identity matrix representing the real unit, and the second of which represents the imaginary unit of the dual number ε (thus, there are two different matrix representations of this imaginary unit ε). Each of the sets of these two matrices is closed under multiplication and corresponds to the multiplication table of the algebra of dual numbers shown in Figure 22.

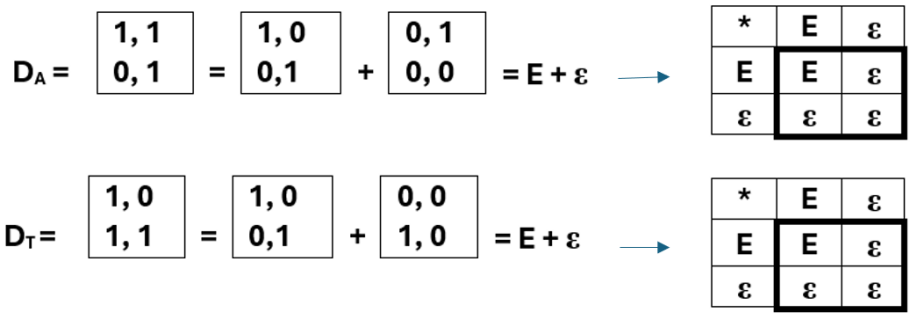

Figure 22. Decomposition of the (2•2)-matrices $\mathbf{D}_A$ and $\mathbf{D}_T$ (from the quadrants along the second diagonal of the genetic (4•4)-matrix of Table 3) shows that they are matrix representations of dual numbers; the multiplication table of their algebra is shown on the right.

What is additionally interesting and unexpected is that the product of these two genetic matrix representations of the dual numbers $\mathbf{D}_T$ and $\mathbf{D}_A$ (Figure 23) yields the Fibonacci matrix $\mathbf{F}$ to the second power (shown in Figure 21), that is, these genetic operators of dual numbers are structurally related to the patterns of inherited phyllotaxis.

$$\mathbf{D}_T * \mathbf{D}_A = \begin{bmatrix} 1, 0 \\ 1,1 \end{bmatrix} * \begin{bmatrix} 1, 1 \\ 0, 1 \end{bmatrix} = \begin{bmatrix} 1, 1 \\ 1, 2 \end{bmatrix} = \mathbf{F}^2$$

Figure 23. The product of the alphabetic-genetic matrices of dual numbers $\mathbf{D}_T$ and $\mathbf{D}_A$ yields the square of the Fibonacci matrix $\mathbf{F}^2$.

The matrix $\mathbf{D}_C = [0, 0; 0, 1]$, which appears in the upper-left quadrant of the (4•4)-matrix in Table 3, is a projection operator, since it satisfies the criterion for such operators: its square is equal to itself. As is well known, projection operators in the screw calculus are a powerful analytical and geometric decomposition tool. They allow the following: to dissect a complex spatial motion or force effect into simple, intuitively understandable components (rotation, translational motion along and across an axis); to work with invariant subspaces, which simplifies mathematical calculations; and to clearly interpret solutions to problems in mechanics and the theory of mechanisms. Without projection operators, the screw calculus would remain just a compact form of notation, but with them, it becomes an effective apparatus for deep geometric analysis. Incidentally, we note that the product of this genetic projector and the Fibonacci matrix to different integer powers generates a matrix operator whose nonzero elements are pairs of adjacent Fibonacci numbers (Figure 24). The manifestation of

© 2025 by the author(s). Distributed under a Creative Commons CC BY license.

Preprints.org (www.preprints.org) | NOT PEER-REVIEWED | Posted: 10 February 2026 doi:10.20944/preprints202512.0208.v2

pairs of adjacent numbers in the Fibonacci sequence is characteristic of phyllotaxis phenomena, for example, the numbers of left and right spiral arrangements of seeds in a sunflower head.

$$\mathbf{D_C}*\mathbf{D_G}^n = \begin{bmatrix} 0, 0 \\ 0, 1 \end{bmatrix} * \begin{bmatrix} 0, 1 \\ 1, 1 \end{bmatrix}^n = \begin{bmatrix} 0, & 0 \\ F_n, & F_{n+1} \end{bmatrix}$$

Figure 24. The product of the alphabetic projector $\mathbf{D_C}$ with the alphabetic Fibonacci matrix $\mathbf{D_G}$ to the power n generates a matrix operator whose non-zero components are adjacent terms of the Fibonacci series (Table 2) like pairs of adjacent numbers in heritable phyllotaxis phenomena.

The author considers the set of these four matrix operators $\mathbf{D_C}$, $\mathbf{D_A}$, $\mathbf{D_T}$, and $\mathbf{D_G}$ as the operator alphabet of a bioinformation system, conventionally termed a spiral-operator bioinformation system (or, for short, "spiral bioinformatics"), for modeling the biological inheritance of spiral structures using the screw calculus. It interacts with the above-discussed unitary-operator bioinformation system (or, for short, "unitary bioinformatics" or "cyclic bioinformatics"), which is based on a related alphabet of four unitary Hadamard operators $\mathbf{H_C}$, $\mathbf{H_A}$, $\mathbf{H_T}$, and $\mathbf{H_G}$ and which is useful for modeling encoded inheritance of cyclic configurations and processes of a pulsating and rhythmic nature. The combined mathematical apparatus of the cyclic and spiral bioinformation systems allows, in particularly, for the modeling of electromagnetic waves with their polarization and other properties, which play an important role in biological organization, including distant communication among the elements of a living body.

Additionally, it is revealed that if we return to Figure 2 and 3, which show four possible arrangements of 4 nucleotides in genetic (2×2) matrices (associated with operators of cyclic bioinformatics), and by analogy algorithmically replace the element -1 with the element 0 in the four binary matrices in Figure 3, we obtain numerical matrices (Figure 25), again associated with Fibonacci numbers and dual numbers of screw calculus, and, therefore, with spiral-operator bioinformatics.

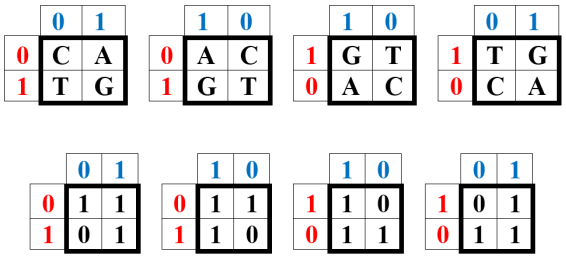

Figure 25. The result of the transformation of 4 genetic Hadamard matrices from Figure 3 by algorithmically replacing the element "-1" with the element "0".

Indeed, the first and third numerical matrices in Figure 25 coincide with the above-discussed matrices $\mathbf{D_A}$ and $\mathbf{D_T}$, representing the dual numbers of the screw calculus. And the second and fourth numerical matrices in Figure 25 are two variants of the Fibonacci matrix $\mathbf{F} = \mathbf{D_G}$ (Figure 21), associated with inherited phyllotaxis spirals.

The action of these alphabetic operators $\mathbf{D_C}$, $\mathbf{D_A}$, $\mathbf{D_T}$, $\mathbf{D_G}$ (as well as the action of their combinations in forms of block matrices and tensor families of operators) on vectors, certainly deserves systematic study in connection with the emerging possibilities for modeling encoded inheritance of biological phenomena. In particular, the identification of the structural connection between the molecular-genetic system and the screw calculus allows one to use those aspects of the screw calculus that are associated with the operators of spiral bioinformatics for the purposes of modeling and comparative analysis of a multitude of inherited spiral forms, for example, the helical three-dimensional configurations of mollusk shells, long used in the theme of "the beauty of natural forms" [Haeckel, 1899; Haeckel, 2007]. The screw calculus allows for the efficient modeling of spiral biological forms, and the results of such modeling can be visualized using publicly available

© 2025 by the author(s). Distributed under a Creative Commons CC BY license.

Preprints.org (www.preprints.org) | NOT PEER-REVIEWED | Posted: 10 February 2026 doi:10.20944/preprints202512.0208.v2

computer tools such as Desmos Graphing Calculator (3D), GeoGebra 3D Graphing Calculator, Wolfram | Alpha, etc.

Figure 26. The single-celled organism *Mixotricha Paradoxa* moves efficiently thanks to the coordinated beating of the spiral flagella of 250,000 bacteria on its surface (image from https://commons.wikimedia.org/wiki/File:Mixotricha_paradoxa_color_and.png, which permits copying and distribution under a Creative Commons Attribution-Share Alike 4.0 International license).

5. Regarding a Combined Cyclo-Spiral Bioinformatics

Many code-inherited biological phenomena are structurally organized in such a way that they bear the characteristics of logically coordinated cyclical and spiral processes. Examples of this include the growth cyclic processes of spiral phyllotaxis in plants and other organisms; the pulsating spiral movement of blood in the cardiovascular system; the cyclical movements of the legs in animal locomotion (including humans and centipedes), and so on. A striking example of the logical interaction of cyclical and spiral bioinformatics is provided by the single-celled organism *Mixotricha Paradoxa* (https://ru.wikipedia.org/wiki/Mixotricha_paradoxa) : it moves thanks to 250,000 spiral-shaped *Treponema spirochetes* bacteria located on its surface, whose spiral flagella work in a coordinated manner as a single unit, ensuring the organism's purposeful movement in the desired directions and speeds through logical interactions and logical control (Figure 26).

Moreover, this organism has only 4 of its own spiral flagella, the movements of which can specify (encode) the coordinated movements of hundreds of thousands of bacterial spiral flagella on its surface for the said purposeful movement of the entire organism. In other words, these 4 of its own flagella can be considered as members of a specialized 4-element alphabet, the motion parameters of which serve as information signals for the algorithmic specification of logically coordinated beats of the said thousands of bacterial flagella. The physical mechanism of this bioinformation exchange is based on electromagnetic waves and the above-mentioned bioantenna arrays for the emission and reception of these waves using the principles of resonance. The spiral antenna differs from other antennas primarily in that its radiation field has circular polarization. At the same time, as is known, the screw calculus provides an ideal, invariant, and geometrically meaningful language for the theory of electromagnetic waves, revealing the fundamental unity of electric and magnetic fields and elegantly deducing all the key properties of electromagnetic radiation [Arthur, 2011; Hestenes, 2003]. It can be assumed that the structural properties of electromagnetic waves, endowed with polarization and other properties, determine much of the operator-alphabetic foundations of cyclic and spiral bioinformatics. It is not surprising that the alphabetic foundations of algebra-operator bioinformatics presented above are related to the algebraic formalisms of the screw calculus and quantum logic.

The vast array of code-inherited biological phenomena suggests the feasibility of combining both cyclic and spiral bioinformatics systems into a single operator cyclo-spiral (or cyclo-screw) bioinformatics system based on a unified operator alphabet of 8 elements: $\mathbf{H}_C$, $\mathbf{H}_A$, $\mathbf{H}_T$, $\mathbf{H}_G$, $\mathbf{D}_C$, $\mathbf{D}_A$, $\mathbf{D}_T$, $\mathbf{D}_G$. To understand deeply the algebraic properties of living organisms, it seems useful to develop in future a cyclo-spiral (or a cyclo-screw) calculus as a complement to the screw calculus.

The operators $\mathbf{H}_C$, $\mathbf{H}_A$, $\mathbf{H}_T$, $\mathbf{H}_G$ and their tensor powers are represented by unitary Hadamard matrices of the corresponding order. As noted above, the Hadamard matrices are related to complete orthogonal systems of Walsh functions of the corresponding order. Therefore, they are also related to Walsh-Hadamard spectral analysis, cyclic Gray codes, fractal Hilbert curves and other useful tools

© 2025 by the author(s). Distributed under a Creative Commons CC BY license.

Preprints.org (www.preprints.org) | NOT PEER-REVIEWED | Posted: 10 February 2026 doi:10.20944/preprints202512.0208.v2

of digital informatics described in our works [Petoukhov, 2008; Petoukhov, 2024a,b; Petoukhov, He, 2023]. An analysis of the interaction of alphabetic operators of both parts of cyclo-spiral bioinformatics (i.e., the operators $\mathbf{H}_C$, $\mathbf{H}_A$, $\mathbf{H}_T$, $\mathbf{H}_G$ with the operators операторами $\mathbf{D}_C$, $\mathbf{D}_A$, $\mathbf{D}_T$, $\mathbf{D}_G$) reveals a number of interesting results. For example, the matrix resulting from the multiplication of the operators $\mathbf{D}_G$ and $\mathbf{H}_C$, when raised to a power, forms a cyclic group with period 8, that is, $(\mathbf{D}_G{*}\mathbf{H}_C)^n = (\mathbf{D}_G{*}\mathbf{H}_C)^{(n+8)}$. And the second power of the Fibonacci matrix $\mathbf{Q}^2$ = [1, 1; 1, 2] from Figure 21 can be represented in the following form based on the named operator alphabets of genetics: $\mathbf{Q}^2 = (\mathbf{D}_G{*}\mathbf{H}_G){*}(\mathbf{D}_G{*}\mathbf{H}_G)^T$, where the symbol T means transposition. When multiplying matrices from these different alphabets, sometimes matrices arise that do not coincide with the classical Fibonacci matrix, but all of whose components are numbers of the Fibonacci series, for example, $\mathbf{D}_G\text{^}5 {*}\mathbf{H}_A{*}2^{0.5}$ = [2, 8; 3, 13].

Let us briefly mention another important matrix representation of the binary-oppositional feature of molecular genetic coding, the consideration of which again leads to the algebraic operators of the cyclic and spiral alphabets of genetics. We are talking about the well-known binary-oppositional feature of the genetic code of amino acids, according to which the set of 16 nucleotide duplets consists of two equal subsets: 8 “strong” duplets (CC, CT, CG, TC, AC, GC, GT, GG) and 8 “weak” duplets (all other duplets); these duplets divide the entire set of 64 triplets encoding amino acids into subsets of 32 triplets with strong roots and 32 triplets with weak roots, each with different coding properties [Rumer, 1968; Fimmel, Strüngmann, 2016; Petoukhov, 2008; Petoukhov, He, 2023]. This binary-oppositional feature is reflected in the author’s previously published black-and-white mosaic matrices of 16 duplets and 64 triplets, in which the meander alternation of signs corresponds to Rademacher functions (the author conditionally calls these mosaic matrices “Rademacher genetic matrices”). Figure 31 shows such a genetic matrix of 16 duplets from Figure 4, in which strong (weak) duplets are now highlighted in black (white). Representing in this matrix of binary opposition the strong (black) duplets by the symbol +1, and the weak (white) duplets by the symbol -1 or the alternative symbol 0, we obtain two related (4•4)-matrices, the quadrants of which contain the (2•2)-matrix operators of genetics described above: the quadrants of the first of them (in the middle of Figure 31) contain Hadamard matrices from the cyclic operator alphabet, and the quadrants of the second matrix (on the right in Figure 27) contain matrix representations of dual numbers and projectors corresponding to the spiral operator alphabet of genetics.

	00	01	10	11
00	CC	CA	AC	AA
01	CT	CG	AT	AG
10	TC	TA	GC	GA
11	TT	TG	GT	GG

	00	01	10	11
00	+1	-1	+1	-1
01	+1	+1	-1	-1
10	+1	-1	+1	-1
11	-1	-1	+1	+1

	00	01	10	11
00	+1	0	+1	0
01	+1	+1	0	0
10	+1	0	+1	0
11	0	0	+1	+1

Figure 27. Rademacher’s genetic matrix of 16 nucleotide duplets (left) and its numerical representations, in which strong (black) duplets are represented as +1 and weak (white) duplets are represented as -1 (middle matrix) or alternatively as 0 (right matrix).

6. Crystal Lattices and Bioinformation Inheritance of Biostructures

The importance of considering ensembles of spiral (helical) bioantennas in connection with the doctrine of energy-informational evolution based on bioantenna arrays as a fundamental inherited tool for communication between the elements of a living organism, as well as between the organism and the outside world, has already been noted above [Petoukhov, 2022]. Crystals are widely used in antennas for electronics and photonics, including aperiodic crystals (quasicrystals), the structures of which make it possible to create microwave emitters, waveguides, and high-density data storage systems. Schrödinger called chromosomes aperiodic crystals [Schrödinger, 1972]. The relationship between molecular genetic informatics and crystal lattices, which can be molecular, atomic, ionic, and metallic, deserves special attention. It is known that the application of the screw calculus to the

© 2025 by the author(s). Distributed under a Creative Commons CC BY license.

Preprints.org (www.preprints.org) | NOT PEER-REVIEWED | Posted: 10 February 2026 doi:10.20944/preprints202512.0208.v2

analysis of crystal lattices led to the development of a scientific school of parallel structure mechanisms for robotics and other fields at the Russian Academy of Sciences [Glazunov, 2010]. The DNA double helix can be viewed as a molecular crystal lattice. Photonic crystals, which also manifest themselves in inherited bodily structures, such as the colored patterns on butterfly wings, are important participants in the organization of molecular genetic informatics [Hu, Petoukhov, Petukhova, 2018]. Some hybrid crystals, when exposed to laser light, behave similarly to neurons in the brain: their response to light is analogous to the response of neurons to a stimulus [Bachinin, Marunchenko, Matchenya, et al., 2024].

The author notes the existence of striking parallels between the organization of the molecular genetics of inheritance of chiral (enantiomorphic) biostructures and the recently discovered Hopfion crystals, which are constructed using antenna-based emitters of light energy [Lin, Mata-Cervera, Ota, Shen, Iwamoto, 2024, 2025]. These Hopfion crystals are nodal structures of light that repeat orderly not only in space but also in time. The key to constructing such light crystals is a two-color light field, the electric vector of which changes its polarization state over time. By carefully superimposing light beams with different spatial modes and opposite circular polarizations, the team creates a "pseudospin" that evolves in a controlled rhythm. When two colors are related in a simple manner, the field pulsates with a fixed period, creating a chain of hopfions that repeats with each cycle. These devices form a distinct spatiotemporal pattern that remains stable even under external influences. Hopfion optical crystals represent a new platform for transmitting topological information in multidimensional space. New aspects of the physics of light-matter interactions are being discovered, related to the development of methods for trapping atoms and molecules.

In the aforementioned pioneering work, the authors say nothing about the parallelisms between Hopfion crystals and the structures of genetic inheritance mechanisms. However, the author of this article believes it is essential, for a deeper understanding of biological informatics and evolutionary biology, to highlight the existence of the following impressive parallelisms:

- The DNA double helix consists of two helical strands of opposite direction (one strand has a direction from the 5'-end to the 3'-end, and the complementary one from the 3'-end to the 5'-end), and Hopfion crystals are produced by superimposing two light beams of opposite circular polarization on each other;
- The genetic system of inheritance has amazing noise-immunity in the inheritance of complex structures from parents in children, and Hopfion crystals have clear spatio-temporal patterns that are preserved under external influences;
- The inherited organization of living bodies is permeated with cyclical (rhythmic) structures of spatial and temporal type, and analogically hopfion crystals exist cyclically in space and time;
- The inherited organization of all living bodies at various levels is characterized by the presence of different chiral enantiomorphic features (i.e. the absence of mirror equality between parts of the organism or molecular structures, usually referred to as biological dissymmetry), which can emit electromagnetic waves of different polarization, and Hopfion crystals are generated by a pair of light rays of different circular polarization (i.e. different chirality);
- Configuration spaces of multiparametric living bodies are multidimensional, and light Hopfion crystals provide a new platform for transmitting topological information in multidimensional spaces;
- Living organisms grow during ontogenesis by incorporating atoms and molecules from food into their body composition, and light-based hopfion crystals open up new aspects of the interaction of light and matter with the possibility of developing new methods for capturing atoms and molecules.

This structural connection between genetic informatics and Hopfion crystals, noted here by the author, draws our attention to ancient ideas about the key role of light waves in living nature and about living bodies as entities woven from light. It is no coincidence that photosynthesis is the fundamental biological process that sustains life on Earth: it converts solar energy into the chemical

© 2025 by the author(s). Distributed under a Creative Commons CC BY license.

Preprints.org (www.preprints.org) | NOT PEER-REVIEWED | Posted: 10 February 2026 doi:10.20944/preprints202512.0208.v2

energy of organic matter, produces oxygen for respiration, and absorbs carbon dioxide, forming the basis of food chains. It is also known that God is associated with light in various religions.

In connection with the consideration of organisms as inherited vast ensembles of coordinated cyclical processes, we will also touch on the topic of "time crystals," which have been actively developed by global science in recent years. Time crystals represent a special state of matter in which particles are in constant motion, creating patterns that repeat over time. The idea of such structures was first proposed by Nobel laureate F. Wilczek in 2012. He then posed the question: if ordinary crystals, such as diamonds or salt, have a spatially ordered structure, is it possible to create a crystal whose structure is also ordered over time? A recent article in the journal Nature Materials [Zhao, Smalyukh, 2025] presents a version of such time crystals that can be directly observed under a microscope and even with the naked eye. These are experimental liquid crystals in which, when exposed to light, stable patterns emerge and begin spontaneous cyclic, soliton-like motion. This motion can continue without ceasing for hours, demonstrating remarkable stability even with changing temperatures. Living bodies contain a multitude of liquid crystals: DNA and RNA, cell membranes, many proteins, and so on are all liquid crystals. Therefore, it can be assumed that the topic of time crystals on liquid crystals is directly related to genetically inherited ensembles of cyclic processes in living organisms and, accordingly, to the quantum-logical bioinformatics models based on genetic unitary operators discussed in our article.

7. Some Concluding Remarks

In a quantum-logical approach to bioinformatics, taking into account the cyclical (or pulsating) properties of living bodies, the author relies on a model representation of biomechanical environments as consisting of interconnected pulsating structures that change in a coordinated manner over time. The theory of such model software environments can be used in the development of artificial intelligence, including in connection with pulsating information lattices (pulsers) known in computer architectures [Guzik, Shmoylov, Kirichenko, 2014]. The name "pulsating" reflects the essence of this architecture, traditionally compared to a heartbeat or pulse. The pulsation appears as a wave of data, and the computational process appears as the propagation of waves of activity. Data received at the inputs of the lattice begin to "pulsate" through it, being transformed at each step. The lattice can be configured so that different data streams collide and interact within specific cells at precisely defined intervals, generating a new "pulse" of results. This architecture is fundamentally different from the von Neumann architecture of conventional processors because it lacks a central control unit; all cells operate simultaneously and synchronously; data is not written in the classical sense, but continuously "pulses" through the processor structure, like blood flow through capillaries. The operation of such a pulsating information lattice is compared to the work of the heart: the lattice is compared to the muscle tissue of the myocardium; the processing elements are compared to individual muscle cells of the heart (cardiomyocytes); the heartbeat is compared to the electrical impulse from the sinoatrial node; calculations are compared to the coordinated contraction of the heart pumping blood; and the information data is compared to the pumped blood.

In this case, the "computation" (blood pumping) is an emergent property of the entire organ, pulsating in a coordinated rhythm; no single cell is responsible for it, but all cells follow the general rhythm and local interactions. Enormous problems in programming and hardware have prevented pulsating information lattices from becoming widespread, the most famous example of the implementation of the pulser concept is the Connection Machine, developed by Thinking Machines Corporation in the 1980s. It had up to 65,536 simple one-bit processors connected in a hypercubic network. The concept of pulsers is also closely related to a number of modern architectural concepts, for example, the concept of systolic arrays, whose name comes from the analogy of their pulse-like operation with cardiac systoles [Kung, Leiserson, 1980; Li, Gao, Chen, et al., 2015; Abramavicius, Mathé, Velikova, et al., 2015]. [2025].

Systolic arrays are extremely effective in artificial intelligence, image processing, pattern recognition, computer vision, and other tasks that animal brains excel at. An example is Google's

© 2025 by the author(s). Distributed under a Creative Commons CC BY license.

Preprints.org (www.preprints.org) | NOT PEER-REVIEWED | Posted: 10 February 2026 doi:10.20944/preprints202512.0208.v2

Tensor Processing Unit (TPU), which uses a large two-dimensional systolic array to perform the massive matrix multiplications required for neural networks with high efficiency. Cardiac systoles are not simply cyclic structures, but cyclo-spiral biological structures with blood helical movements in pulse regime. In light of this, the potential development of systolic processors by transition from cyclic to cyclo-spiral algorithms is emerging.

The algebraic bioinformatics presented in this article explains the rapid evolution of organisms by the following thought: complex tissues are formed not so much by the emergence of new genes as by algebraic bioinformatics, whose operators alter the use of existing genes being connected with electromagnetic and resonance mechanisms. In light of this, the author proposes a paradigm of "**code algebraic-operator Darwinism**," according to which natural selection and the inheritance of the most beneficial code combinations for survival play a key role in evolution, based on the alphabetic operators of algebraic bioinformatics. One example that supports the proposed paradigm of code algebraic-operator Darwinism is the "iron" snail *Chrysomallon squamiferum*, whose shell is made of iron and sticks to a magnet (Figure 28). Only 11% of its genes are unique. The remaining 89% are reused ancient genes that existed in the common ancestors of mollusks more than 540 million years ago [Yao et al., 2010].

Figure 28. This photo of *Chrysomallon squamiferum* is reproduced from Wikipedia (https://commons.wikimedia.org/wiki/File:Chrysomallon_squamiferum_2.png), it is licensed under the Creative Commons Attribution 2.5 Generic license.

We briefly note that algebraic bioinformatics formalisms also allow for comparative analysis of relatively short genetic sequences (e.g., DNA sequences of genes) and also the consideration of time-dependent genetic matrix operators. These issues are beyond the scope of this article and merit a separate publication.

The described algebraic-operator bioinformatics seems to be useful for the analysis of gene networks and related problems [Kolchanov, Vishnevsky, Furman, 2015]. It is linked to the actively developing topic of code biology [Barbieri, 2015]. Annual international conferences are held on this code topic, and the International Code Biology Society (https://www.codebiology.org/) operates. An important component of the formalisms of this algebraic-operator bioinformatics are tensor-unitary transformations, which provide an increase in the dimensionality of configuration vector Hilbert spaces in quantum logical models of growing biological systems [Petoukhov, 2025].

The history of science attests to the particular importance of the search for cognitive forms of representing phenomenological data, that is, condensed and analytically convenient forms of representing countless units of information about nature systems. The entire development of mathematical natural science is largely based on the discovery of such forms. A classic example is the work of Kepler, who, without conducting his own astronomical observations, managed to find a unique form of representing the difficult-analyzed astronomical data on planetary motion from the ledgers of Tycho Brahe. This cognitive form he discovered, linked to the generalizing idea of elliptical motion, allowed him to formulate the laws of planetary motion relative to the Sun, which became known as Kepler's laws.

Thanks in large part to the discovery of this cognitive form, many years later, another person—Newton—formulated the law of universal gravitation. In biology, the search for a similar cognitive form of representing the difficult-to-understand set of units of experimental information has long

© 2025 by the author(s). Distributed under a Creative Commons CC BY license.

Preprints.org (www.preprints.org) | NOT PEER-REVIEWED | Posted: 10 February 2026 doi:10.20944/preprints202512.0208.v2

been urgent. This work is part of the search for such a cognitive mathematical form of representing code-inherited biological ensembles of algorithmic sets of elements. The development of algebra-operator bioinformatics additionally contributes to the uncovering of the mathematical unity of animate and inanimate nature, as this bioinformatics is based on a mathematical apparatus that plays an important role in the physical sciences as it is well-known.

The author believes it is useful to formulate a number of programmatic tasks for the theoretical and applied development of this algebra-operator bioinformatics as part of algebraic biology [Petoukhov, 2008; Petoukhov, He, 2023]:

- In-depth development of the biomathematical foundations of the aforementioned paradigm of code algebra-operator Darwinism;
- Analysis and interpretation of the principles and laws of Mendelian genetics from the perspective of algebra-operator bioinformatics;
- Analysis of code-inherited biological fractals and their development during ontogenesis from the perspective of algebra-operator bioinformatics;
- Development (with consideration of algebra-operator bioinformatics) of the topic of chirality in living organisms in connection with code-inherited ensembles of spiral and spiral-fractal bioantennas that generate and receive circularly polarized waves (having significant advantages in communications technology);
- Development of genetic algorithms and the theory of genetic automata, taking into account algebra-operator bioinformatics;
- Analysis of the relationship between algebra-operator bioinformatics and genetic archetypes and C. Jung's theory of the archetypes of the collective unconscious, as well as the philosophical concepts of Ancient China and Ancient India;
- Analysis of the relationship between the Hardy-Weinberg law of population genetics and algebra- operator bioinformatics;
- Analysis (from the perspective of algebra-operator bioinformatics) of parallelisms between the molecular genetics of structural inheritance and Hopfion crystals.

Acknowledgments: A number of the results in this article were achieved thanks to long-term collaboration between the Russian and Hungarian Academies of Sciences on the topic "Nonlinear Models and Symmetrological Analysis in Biomechanics, Bioinformatics, and Theory of Self-Organizing Systems," for which the author served as the scientific advisor from the Russian Academy of Sciences. The author thanks V.I. Chernoivanov, E. Fimmel, M. He, S.Ya. Kotkovsky, Yu.I. Manin, V.I. Svirin, I.V. Stepanyan, and G.K. Tolokonnikov for their collaboration.

Comment: Some materials of this article were presented by the author in his talks at the First China-Russia Symposium on Artificial Intelligence and Quantum Computing (18.01.2025, Shenzhen, China); International Conference "Mathematics of Artificial Intelligence" (24-28.03.2025, Sochi, Russia, https://openreview.net/group?id=mathai.club/MathAI/2025); International Conference "Science and Spirituality for Global Peace and Harmony (IAPIC-2025)" (09-12.04.2025, Hyderabad, India, https://www.iapic.net/); XXI Conference "Finsler Generalizations of the Theory of Relativity" (FERT-2025) (12-13.12.2025, Moscow, Russia); IX Russian Conference "Foundations of Fundamental Physics and Mathematics" (OFFM-2025)" (19-20.12.2025, Moscow, Russia); International Conference "Hyderabad Artificial Conference 2025" (29-30 November, Hyderabad, India, https://iaic.world/conferences/2025_india_hyderabad.html).

References

Abbott D., Davies P.C.W., Pati A.K. eds. Quantum Aspects of Life (foreword by Sir Roger Penrose). - World Scientific, 2008.

Abramavicius V., Mathé M., Velikova G.V., et al. PulserDiff: a pulse differentiable extension for Pulser. - arXiv:2505.16744v1 from 22.05.2025, https://doi.org/10.48550/arXiv.2505.16744

© 2025 by the author(s). Distributed under a Creative Commons CC BY license.

Preprints.org (www.preprints.org) | NOT PEER-REVIEWED | Posted: 10 February 2026 doi:10.20944/preprints202512.0208.v2

Arthur J.V. Understanding Geometric Algebra for Electromagnetic Theory. – 2011, Print ISBN:9780470941638 |Online ISBN:9781118078549 |DOI:10.1002/9781118078549.

Asano M., Basieva I., Khrennikov A, et al. A model of epigenetic evolution based on theory of open quantum systems. Syst Synth Biol, 2013, 7:161–173. doi:10.1007/s11693-013-9123-2.

Astashkin S.V. Rademacher system in functional spaces. Moscow: Fizmatlit, 2017. 552 p. ISBN 978-5-9221-1703-6 (in Russian).

Balonin N.A., Sergeev A.M. Hadamard matrices with symmetries in illustrations. Monograph. SPb.: GUAP, 2024 (in Russian).

Bank E. How much time does it take for a DNA molecule to replicate? Sciencing. 2022, https://sciencing.com/much-time-dna-molecule-replicate-21660.html.

Barbieri M. Code Biology. A New Science of Life. Springer-Verlag, 2015. ISBN 978-3-319-14534-1, doi 10.1007/978-3-319-14535-8.

Bachinin S.V., Marunchenko A., Matchenya I. et al. Metal-organic framework single crystal for in-memory neuromorphic computing with a light control. *Commun Mater* **5**, 128 (2024). https://doi.org/10.1038/s43246-024-00573-6

Baydin A.G., Pearlmutter B.A., Radul A.A., Siskind J.M. Automatic differentiation in machine learning: a survey. The Journal of Machine Learning Research, 18(153):1--43, 2018. https://arxiv.org/abs/1502.05767.

Birkhoff G., von Neumann J. The Logic of Quantum Mechanics, 1936, vol 37, 823—843.

Bodnar O.Ya. Golden Ratio and Non-Euclidean Geometry in Nature and Art. Lviv: Publishing House "Sweet", 1994.

Bodnar O.Ya. The geometry of phyllotaxis. Reports of the Academy of Sciences of Ukraine. 1992, №9, p. 9-15

Carlevaro C.M., Irastorza R.M., Vericat F. Quaternionic representation of the genetic code. - Biosystems, Volume 141, 2016, Pages 10-19, ISSN 0303-2647, **https://doi.org/10.1016/j.biosystems.2015.12.009.**

Chernoivanov V.I., Petukhov S.V., Rajan E.G., Tolokonnikov G.K. Systems approach and artificial intelligence in agricultural engineering. - V International Kosygin Forum. Collection of scientific papers of the International Scientific and Technical Symposium "Modern Engineering Problems of Key Sectors of the Economy" (October 15-16, 2025). Vol. 1. Pp. 43-47. - M.: RSU im. A.N. Kosygin, 2025.

Cohen D. An Introduction to Hilbert Space and Quantum Logic. - Springer-Verlag, 1989.

Cook T.A. The curves of life. -L., Constable and Co., 1914, 490 p.

Decker J.A. Jr., **Harwitt M.O**. Sequential encoding with multislit spectrometers. Appl Opt. 1968 Nov 1;7(11):2205-9. doi: 10.1364/AO.7.002205. PMID: 20068968.

Dimentberg F.M. Screw calculus and its applications in mechanics. – Moscow, Nauka, 1965 (In Russian; English translation - https://www.dma.unifi.it/~minguzzi/Dimentberg65%20-%20The%20screw%20calculus%20and%20its%20applications%20in%20mechanics.pdf).

Dragunsky V.V. Color personality test: a practical guide. - Minsk: Harvest, 2001, 448 p. (in Russian).

Eigen M., **Schuster P**. The Hypercycle. A Principle of Natural Self-Organization // Springer-Verlag Berlin Heidelberg New York, 1979. (на русском: Эйген М., Шустер П. Гиперцикл. Принципы самоорганизации макромолекул. - М.: Мир, 1982.

Fimmel E., Gumbel M., Karpuzoglu A., Petoukhov S. On comparing composition principles of long DNA sequences with those of random ones. – *Biosystems*, v. 180, pages 101-108, June 2019.

Fimmel E., Michel Ch. J., Pirot F., Sereni J-S., Strüngmann L. Mixed circular codes, Mathematical Biosciences Volume 317, November 2019, 108231. https://doi.org/10.1016/j.mbs.2019.108231.

Fimmel E., Strüngmann L. Yury Borisovich Rumer and his 'biological papers' on the genetic code. - Phil. Trans. R. Soc. A, 2016, 374. (http://dx.doi.org/10.1098/rsta.2015.0228).

Fimmel E., Starman M., Strüngmann L. Circular Tessera Codes in the Evolution of the Genetic Code, Bull Math Biol 82, 48, 2020, https://doi.org/10.1007/s11538-020-00724-z. **Fimmel E., Michel C.J., Pirot F., Sereni J.-S., Starman M., Strüngmann L**. The Relation Between k-Circularity and Circularity of Codes. Bull Math Biol 82, 105, 2020. https://doi.org/10.1007/s11538-020-00770-7.

Glazunov V.A., Kostereva S.D., Danilin P.O., Lastochkin A.B. Application of screw calculus in the modern theory of mechanisms. - Bulletin of Scientific and Technical Development. 2010, No. 6 (34), www.vntr.ru, https://www.vntr.ru/ftpgetfile.php?id=426 (in Russian).

© 2025 by the author(s). Distributed under a Creative Commons CC BY license.

Preprints.org (www.preprints.org) | NOT PEER-REVIEWED | Posted: 10 February 2026 doi:10.20944/preprints202512.0208.v2

Gordeev V.N. Quaternions and biquaternions with applications in geometry and mechanics. – Kyiv: Stal Publishing House, 2016. – 316 p. ISBN 978-617-676-099-3 (in Russian).

Gsponer A., Hurni J.-P. Quaternions in mathematical physics (2): Analytical bibliography. -arXiv:math-ph/0511092v3 , 124 pages, from 6 July 2008, https://doi.org/10.48550/arXiv.math-ph/0511092.

Gusfield D. Algorithms on Strings, Trees, and Sequences: Computer Science and Computational Biology. - Cambridge University Press, 1997.

Guzik V.F., Shmoilov V.I., Kirichenko G.A. Pulsating information grids with matrix switching. - News of universities. North Caucasian region. Series: Technical sciences. 2014. No. 6 (181), pp. 3-12. DOI: 10.17213/0321-2653-2014-6-3-11. URL: https://cyberleninka.ru/article/n/pulsiruyuschie-informatsionnye-reshyotki-s-matrichnoy-kommutatsiey (in Russian).

Haeckel E. Kunstformen der Natur. – Leipzig und Wien, Bibliographisches Institut, 1899.

Haeckel E. Beauty of Forms in Nature. - St. Petersburg: Werner Regen Publishing House, 2007.144 p. ISBN 5-903070-08-6 (in Russian).

Hesse H. The Glass Bead Game. -Penguin. Hammondsworth, 1975.

Hestenes D. Oersted Medal Lecture 2002: Reforming the mathematical language of physics. – American Journal of Physics, 2003, 71(2):104-121, DOI:10.1119/1.1522700

Hu Z, Petoukhov SV, Petukhova ES. On symmetries, resonances and photonic crystals in morphogenesis. Biosystems. 2018 Nov;173:165-173. doi: 10.1016/j.biosystems.2018.09.004. Epub 2018 Sep 14. PMID: 30222993.

Jean R.V. Phyllotaxis: a systemic study of plant pattern morphogenesis. - Cambridge; New York: Cambridge University Press, 1994.

Kantor I.L., Solodovnikov A.S. Hypercomplex numbers. Springer-Verlag, 1989.

Karzel H., Kist G. Kinematic Algebras and their Geometries. In: Rings and Geometry, eds. R. Kaya, P. Plaumann, and K. Strambach, 1985. pp. 437–509.

Khrennikov A. On quantum-like probabilistic structure of mental information. Open Syst Inf Dyn, 2004, 11(3):267–275.

Khrennikov A. Quantum-like brain: interference of minds. BioSystems, 2006, 84: 225–241.

Kienle G. Experiments concerning the non-euclidian structure of the visual space. – In: Bioastronautics. N.Y., London, 1964, p. 386-400.

Kisil V.V. Inventing the Wheel, the Parabolic One. - 2007, arXiv:0707.4024.

Kolchanov N.A., Vishnevsky O.V., Furman D.P., editors. Introduction to Information Biology and Bioinformatics: a textbook in 5 volumes; Novosibirsk State University. - Novosibirsk: RIC NSU, 2015. - Vol. 3. - 298 p.

Kung H.T., Leiserson C.E. Algorithms for VLSI Processor Arrays. - in *Introduction to VLSI Systems*, C. Mead and L. Conway (eds.), Addison-Wesley, 1980, Sect. 8.3.

Li, H., Gao, B., Chen, Z. et al. A learnable parallel processing architecture towards unity of memory and computing. *Sci Rep* **5**, 13330 (2015). https://doi.org/10.1038/srep13330.

Lieberman-Aiden E., van Berkum N.L., Williams L., Imakaev M., Ragoczy T., Telling A., Amit I., Lajoie B.R., Sabo P.J., Dorschner M.O., et al. Comprehensive mapping of longrange interactions reveals folding principles of the human genome, Science, 326, 289, 2009.

Lin W, Mata-Cervera N, Ota Y, Shen Y, Iwamoto S. Space-Time Hopfion Crystals. - arXiv:2406.06096v1 [physics.optics], 10 Jun 2024.

Lin W, Mata-Cervera N, Ota Y, Shen Y, Iwamoto S. Space-Time Optical Hopfion Crystals. -Phys Rev Lett. 2025 Aug 22;135(8):083801. doi: 10.1103/hh5s-cprt. PMID: 40929334.

Lobodenko E.I. Quaternion structure of operators describing vibrational-rotational states of molecules. - Bulletin of Tyumen State University, 2009, No. 6, pp. 203-209.

Luneburg R.K. The metric of binocular visual space. J. Opt. Soc. Amer., v. 40, #10, 1950, p. 627-642.

Lüscher M. The Lüscher Color Test / transl. and ed. by Ian A. Scott. — New York : Pocket Books, 1971. — 187 p. — Ориг. изд. Random House, 1969. — ISBN 0671-78073-5.

Manin Yu.I. Computable and Uncomputable. Moscow, Soviet Radio, 1980, 128 p. (in Russian).

© 2025 by the author(s). Distributed under a Creative Commons CC BY license.

Preprints.org (www.preprints.org) | NOT PEER-REVIEWED | Posted: 10 February 2026 doi:10.20944/preprints202512.0208.v2

Mumford D., Series C., Wright D. Indra's Pearls. The Vision of Felix Klein by David Mumford, Caroline Series, and David Wright. Cambridge University Press, 2002.

Niall K.K., ed. Erwin Schrödinger's Color Theory: Translated with Modern Commentary / Ed. K. K. Niall. Cham: Springer, 2017. 193 p. DOI: 10.1007/978-3-319-64621-3 - (Шредингер Э. Основные принципы метрики цветов в дневном свете. – Новые пути в физике. Статьи и речи. – М., Наука, 1971, стр. 135-192).

Nielsen M.A., Chuang I.L. Quantum Computation and Quantum Information, (Cambridge Univ. Press, 2010) (https://doi.org/10.1017/CBO9780511976667)

Patel A. Quantum algorithms and the genetic code, Journal of Physics, 2001a, v. 56, 2-3, pp. 367-381. (arXiv:quant-ph/0002037).

Patel A. Why genetic information processing could have a quantum basis. - Journal of Biosciences, 2001b, v. 26, 2, pp. 145-151.

Petoukhov S.V. Non-Euclidean geometries and algorithms of living bodies. – Computers & Mathematics with Applications, v. 17, № 4-6, 1989, p. 505-534.

Petoukhov S.V. Matrix genetics, genetic code algebras, noise immunity. – M., RKhD, 2008, 316 p. https://petoukhov.com/matrix-genetics-petoukhov-2008.pdf. (in Russian).

Petoukhov S.V. The stochastic organization of genomes and the doctrine of energy-information evolution based on bio-antenna arrays. *Biosystems*, 2022, 104712, ISSN 0303-2647, https://doi.org/10.1016/j.biosystems.2022.104712.

Petoukhov S.V. The principle "like begets like" in algebra-matrix genetics and code biology. Biosystems, 233 (2023) 105019.

Petoukhov S.V. The Doctrine of Energy-Information Evolution Based on Bio-Antenna Arrays and Algebraic Biology. – Selected Proceedings of the World Congress "Systems Theory, Algebraic Biology, Artificial Intelligence", June 26-30, 2023, Moscow (https://congrsysalgbai.ru/), 2023, pp. 343-358. DOI 10.18699/sblai2023-62.

Petoukhov S. Cyclic Gray Codes in Modeling Inherited Cyclic Biostructures and Analysis of Statistical Rules of Genomic DNAs. – Preprints 2024, 2024020713, 2024a, 40 pages, https://doi.org/10.20944/preprints202402.0713.v1.

Petoukhov S.V. Genetic code, the problem of coding biological cycles, and cyclic Gray codes. – Biosystems, vol. 246, December 2024b, 105349, https://doi.org/10.1016/j.biosystems.2024.105349 .

Petoukhov S.V. Genetic intelligence and tensor-unitary transformations. - System Informatics, № 27, 2025, p. 1-14, DOI 10.31144/si.2307-6410.2025.n27.p1-14 (https://system-informatics.ru/article/372, https://system-informatics.ru/en/article/372

Petoukhov S.V., He M. Algebraic biology, matrix genetics, and genetic intelligence. - Singapore, World Scientific, 2023, 616 p., https://doi.org/10.1142/13468.

Petoukhov S.V., He M. Symmetrical Analysis Techniques for Genetic Systems and Bioinformatics: Advanced Patterns and Applications. Hershey, USA, IGI Global, 2010.

Petoukhov S.V., Svirin V.I. Binary-genomic numbers and symmetrical regularities in the statistical organization of genomic DNAs. – Symmetry: Culture and Science, 2024, №4, p.469-492.

Petoukhov S.V., Svirin V.I., Khazina L.V. Bionics of Spiral Structures. – Journal of Machinery Manufacture and Reliability, 2015, Vol. 44, No. 3, pp. 249–253. © Allerton Press, Inc., 2015. https://petoukhov.com/Bioinics_of_Spiral_Structures_2015_Petoukhov.pdf.

Prasolov V.V. Problems and theorems of linear algebra. 2nd ed. - M., RKhD, 2008, 536 p. (in Russian).

Press release. The Nobel Prize in Physiology or Medicine 2017. https://www.nobelprize.org/prizes/medicine/2017/press-release/

Rebrova I.M., Rebrova O.Yu. Memory devices based on artificial DNA: birth of the idea and first publications. - Questions in the History of Natural Science and Technology. 2020. Vol. 41. No.4. Pp. 666–676. DOI: 10.31857/S020596060013006-8 (in Russian).

Rumer Yu. B. Codon systematization in the genetic code. - Doklady Akademii Nauk SSSR, 1968, 183(1), pp. 225-226.

Schillinger J. Baker's Biografical Fictionary of Musicians (англ.) / Completely Revised by Nicolas Slonimsky. — Fifth Edition. — New York: G. Schirmer Inc., 1958. P. 1438.

© 2025 by the author(s). Distributed under a Creative Commons CC BY license.

Preprints.org (www.preprints.org) | NOT PEER-REVIEWED | Posted: 10 February 2026 doi:10.20944/preprints202512.0208.v2

Schrodinger E. What is life? The physical aspect of the living cell. Cambridge University Press, 1955.

Smolyaninov V.V. Spatio-temporal problems of locomotion control. Uspekhi Fizicheskikh Nauk, 2000, v.170, N 10, p. 1063–1128, DOI: https://doi.org/10.3367/UFNr.0170.200010b.1063.

Spasennikov V.V. The phenomenon of color perception in ergonomic research and color consulting. – Ergodesign, vol. 2019, no. 2, 2019, pp. 1-5. DOI: 10.30987/article_5cb22163c8b6b7.59336480 (in Russian).

Steitz T.A. Collecting Butterflies and the Protein Structure Initiative: The Right Questions? - Structure, 2007, Volume 15, Issue 12, 1523 – 1524, DOI 10.1016/j.str.2007.11.005.

Tolmachev Yu.A. New optical spectrometers. L., 1976.

Tsyganok I.I. Color psychodiagnostics. Modification of the complete clinical test of Luscher. - St. Petersburg: Rech, 2007. - 264 p.

Vasyukov V.L. Quantum Logic. - M.: PER SE, 2005, 191 p. ISBN 5-9292-0142-0 (in Russian).

Vetter R.J., Weinstein S., The history of the phantom in congenitally absebt limbs. – Neuropsychologia, 1967, № 5, p.335-338.

Weinstein S., Sersen E.A. Phantoms in cases of congenital absence of limbs. - Neurology, 1961, #11, p.905-911.

Wiener N. People and Machines. The Last Interview of the "Father of Cybernetics" Norbert Wiener // Izvestia (newspaper). Supplement "Week". March 22–28, 1964, No. 13 (213). Pp. 12–13, 20–21.

Wright K. Times of our lives. - Scientific American, Sept., 2002, 58-65.

Xu T., Cheng D., Zhao Y., et all. Polymorphic tandem DNA repeats activate the human telomerase reverse transcriptase gene, *Proc. Natl. Acad. Sci. U.S.A.* 118 (26) e2019043118, https://doi.org/10.1073/pnas.2019043118 , 2021).

Yaglom I.M. Complex numbers and their application in geometry. - Moscow: Fizmatlit, 1963. 192 p. (in Russian).

Yamagishi M.E.B. Mathematical Grammar of Biology. Switzerland, Springer International Publishing AG), 2017.

Yao H., Dao M., Imholt T., Huang J., Wheeler K., Bonilla A., Suresh S., Ortiz C. Protection mechanisms of the iron-plated armor of a deep-sea hydrothermal vent gastropod. - Proc. Natl. Acad. Sci. U.S.A., 2010, 107 (3) 987-992, https://doi.org/10.1073/pnas.0912988107.

Zhao H., Smalyukh I.I. Space-time crystals from particle-like topological solitons. *Nat. Mater.* **24**, 1802–1811, 2025. https://doi.org/10.1038/s41563-025-02344-1. Published 04 September 2025.

Disclaimer/Publisher's Note: The statements, opinions and data contained in all publications are solely those of the individual author(s) and contributor(s) and not of MDPI and/or the editor(s). MDPI and/or the editor(s) disclaim responsibility for any injury to people or property resulting from any ideas, methods, instructions or products referred to in the content.

© 2025 by the author(s). Distributed under a Creative Commons CC BY license.